MiWEBA

Millimetre-**W**ave **E**volution for **B**ackhaul and **A**ccess

EU Contract No. FP7-ICT-608637

WP4: Radio Resource Management for mm-wave Overlay HetNets

D4.1: System Level Simulator Specification

Contractual date:	M18
Actual date:	Dec. 2014
Authors:	See list
Work package:	D4.1 System Level Simulator Specification
Security:	Restricted to other programme participants (including the Commission Services).
Nature:	Report
Version:	1.0
Number of pages:	64

Abstract

This report provides specification of the system level simulator developed in the Work Package 4.1 "Radio Resource Management for mm-wave Overlay HetNets" for systematic evaluation of mm-wave Overlay HetNets. Chapter 1 gives an overview of the developed system architecture, which includes the interfaces with link level simulator. Details on link level simulator of the access link between the base station and mobile terminal are presented in Chapter 2. Chapter 3 describes parameters employed in the system level simulator. Evaluation methods and factors showing the impact of the proposed mm-wave Overlay HetNets are presented in Chapter 4. Preliminary systematic evaluation results are summarized in Chapter 5.

Keywords

mm-wave, link level simulator (LLS), system level simulator (SLS), parameters, evaluation method, performance analysis

Authors

IMC	Maltsev Alexander	alexander.maltsev@intel.com
	Bolotin Ilya	ilya.bolotin@intel.com
	Lomayev Artyom	artyom.lomayev@intel.com
	Pudeyev Andrey	andrey.pudeyev@intel.com
	Ingolf Karls	ingolf.karls@intel.com
AVC	Shozo Okasaka	okasaka.shozo@jp.panasonic.com
POLIMI	Ilario Filippini	ilario.filippini@polimi.it
Osaka Univ	Kei Sakaguchi	sakaguchi@comm.eng.osaka-u.ac.jp
Tokyo Tech	Gia Khanh Tran	khanhtg@mobile.ee.titech.ac.jp
	Hidekazu Shimodaira	shimodaira@mobile.ee.titech.ac.jp
	Ebrahim Rezagah Roya	roya@mobile.ee.titech.ac.jp

Table of contents

Abbreviations **5**

Executive Summary **9**

0 Introduction **10**

0.1 Background for development of system level simulator 10

0.2 Relation to other work packages 10

0.3 Structure of the document 10

1 Simulator architecture **11**

1.1 Overall simulator architecture 11

2 Link level simulator **12**

2.1 Link level simulator for 2GHz and 3.5GHz LTE 12

2.1.1 Link level simulator parameters 12

2.1.2 Evaluation results 12

2.2 Link level simulator for 60GHz WiGig 14

2.2.1 IEEE 802.11ad PHY Layer Overview 15

2.2.2 Link Level Simulation Platform 27

2.2.3 Acquisition Test Description 31

2.2.4 Data Transmission Test Description 36

2.3 Interface between LLS and SLS 39

2.3.1 Physical layer abstraction method 39

2.3.2 Mm-wave PHY abstraction 41

3 System level simulator **45**

3.1 Parameters for system level simulator 45

3.1.1 LTE standard macro and smallcell parameters 45

3.1.2 Mm-wave small cell 46

3.2 Resource management framework 46

3.2.1 Network architecture and C/U splitting 46

3.2.2 Mobility management (cell association for U-plane) 47

3.2.3 Radio resource control 48

3.3 System level simulator 48

3.3.1 SLS procedure 49
3.3.2 Simulations setup 49
3.3.3 SLS core and Loop over frames 53
3.3.4 System level simulator GUI 56

4 Evaluation methodology 57

4.1 Evaluation factors 57

4.2 Simulator calibration 57

5 Preliminary evaluation results 59

5.1 Performance comparison of mm-wave overlay HetNet (Full-buffer scenario) 59

5.1.1 Mm-wave overlay HetNet deployment in Europe and Japan 59
5.1.2 Deployment of mm-wave small cells in the Macro LTE cell 59
5.1.3 System level simulations results. 60

5.2 Performance comparison of mm-wave overlay HetNet (Non-full-buffer scenario) 62

6 References 63

Abbreviations

Acronym	Description
3GPP	3rd Generation Partnership Project
ACK	Acknowledgement
ADC	Analog to Digital Convertor
AGC	Auto Gain Control
APDP	Average Power Delay Profile
ARQ	Automatic Repeat Request
AS	Angular Spread
AWGN	Additive White Gaussian Noise
BER	Bit Error Rate
BLER	Block Error Rate
BRP	Beam Refinement Protocol
BS	Base Station
CDF	Cumulative Distribution Function
CEF	Channel Estimation Field
CFO	Carrier Frequency Offset
CoMP	Coordinated Multipoint Transmission
CP	Cyclic Prefix
C-RAN	cloud RAN
CSI	Channel State Information
BBU	Base Band Unit
C-plane	Control Plane
CPRI	Common Public Radio Interface
CQI	Channel Quality Indicator
CSI	channel state information
CoMP	Coordinated Multi-Point transmission
DAC	Digital to Analog Convertor
DFT	Discrete Fourier Transform
DMG	Directive Multi Gigabit
DS	Delay Spread

EVM	Error Vector Magnitude
FD	Frequency Duplex
FEC	Forward Error Correction
FFT	Fast Fourier Transform
GUI	Graphic User Interface
HARQ	hybrid automatic repeat request
ICIC	Intercell Interference Coordination
IDFT	Inverse Discrete Fourier Transform
IFFT	Inverse Fast Fourier Transform
ISD	Inter-Site Distance
ISS	Initiator Sector Sweep
HetNet	Heterogeneous Network
LA	Link Adaptation
LDPC	Low Density Parity Check
LLR	Log Likelihood Ratio
LLS	Link Level Simulator
LTE	Long Term Evolution
MAC	Media Access Control
MCS	Modulation and Coding Scheme
MeNB	Master e-nodeB
MIMO	multiple-input multiple- output
MMIB	Mean Mutual Information per Bit
MMSE	Minimum Mean Square Error
mm-wave	Millimeter-Wave band (30 to 300 GHz) will be used for 6 to 100 GHz
MS	Mobile Station
MU	Multi-user
NLOS	Non-line-of-sight
OBO	Output Back-off
OFDM	Orthogonal Frequency Division Multiplexing
OFDMA	Orthogonal Frequency Division Multiple Access
PA	Power Amplifier
PDF	Probability Density Function
PDSCH	Physical Downlink Shared Channel

PDU	Protocol Data Unit
PER	Packet Error Rate
PF	Proportional Fair
PHY	Physical layer
PN	Phase Noise
PSDU	PHY Service Data Unit
QAM	Quadrature Amplitude Modulation
RBW	Resolution Bandwidth
RF	Radio Frequency
RRH	Remote Radio Head
RRU	Remote Radio Unit
RRM	Radio Resource Management
RS	Reed Solomon
RSRP	Reference Signal Received Power
RSRQ	Reference Signal Received Quality
RX	Receiver
RXSS	Receive Sector Sweep
SC	Single Carrier
SCME	Spatial Channel Model Extended
SeNB	Secondary e-nodeB
SINR	Signal to Interference and Noise Ratio
SLS	System Level Simulator
SM	Spectrum Mask
SNR	Signal to Noise Ratio
SQPSK	Spread QPSK
SS	Sector Sweep
STF	Short Training Field
TDMA	Time Domain Multiple Access
TX	Transmitter
TXSS	Transmit Sector Sweep
UE	User Equipment
U-plane	User Plane
PoC	Proof of Concept

PL	Path Loss
ZF	Zero Forcing

Executive Summary

Due to the popularization of smart phones and tablets in recent years, the traffic load on conventional cellular networks is predicted to be increased by 1000 times in the next 10 years. To face the severe issue of system capacity shortage due to the increasing data traffic in cellular networks, MiWEBA does pioneering work in evolving mm-wave into future 5G cellular networks by a novel U/C splitting architecture of mm-wave overlay heterogeneous networks. As a measure to validate the effectiveness of our proposed architecture to extend the network capacity to a 1000 times, system level simulators were jointly developed and implemented by WP4 partners. The preliminary versions of the simulators include all fundamental technologies of the proposed novel architecture i.e. U/C splitting which supports global optimization of resources and many mm-wave smallcell BSs overlaid inside the coverage of conventional LTE macro cells. Especially, the developed system level simulators have a useful interface with the link level simulators extracting parameters from the state-of-art mm-wave IEEE 802.11ad access link architecture to guarantee the authenticity of the derived system level results. Moreover, a new mm-wave channel model based on the measurement campaign reported in D5.1 was also adopted into the system level simulators. The first numerical results on both full-buffer scenario in Europe and Japan; and non-full-buffer scenario based on realistic traffic model in Japan show that the proposed novel architecture can definitely support the dramatically increasing data traffic demand in the next 10 years as an effect of introducing sufficient numbers of mm-wave smallcell BSs.

0 Introduction

0.1 Background for development of system level simulator

The goal of MiWEBA project is to integrate the millimeter-wave communication potential into the LTE cellular network framework. In order to accomplish this task a radically new network architecture is required, new functionalities must be developed and new scenarios need to be investigated. Moreover, the novelty and the complexity of the research theme result in a large set of possible design choices.

In the WPs of this project viable solutions are discussed and, among them, the most promising are engineered. However, in order to show the viability of the proposed approaches and to assess the network performance once these techniques are applied, simulation tools must be developed.

This deliverable provides a complete picture of the simulation tools developed and implemented within the project in order to show both the type of simulations being carried out and the evaluation methodology considered. In addition, preliminary simulation results are shown as well.

Due to the complexity of the considered system, two simulation approaches have been pursued, which have led to the development of simulators at two different system scales. First, link level simulators are used to evaluate the performance of the millimeter-wave channel at different frequencies. Second, full system simulators are applied to test the network behavior.

0.2 Relation to other work packages

The simulator tools described in this deliverable are used to evaluate real solutions to the C-/U-plane split issues raised and discussed in *Deliverable D3.1*. Results of simulations activities provide useful insights to the protocol architecture that will be discussed in *Deliverable D3.2*.

Findings on new innovative channel modeling carried out in *Deliverable 5.1* are already included in the simulator tools described in this deliverable. A further document, *Deliverable D4.2*, will show analytical tools to assess the higher-level performance of the proposed solution in general and/or in specific scenarios.

0.3 Structure of the document

Next Section, Section 1, explains the overall simulator architecture. Section 2 describes link level simulators at different carrier frequencies, while Section 3 reports details about system level simulators, exploring their building blocks. Section 4 discusses the evaluation methodology considered in the project, while Section 5 shows related preliminary numerical results.

1 Simulator architecture

1.1 Overall simulator architecture

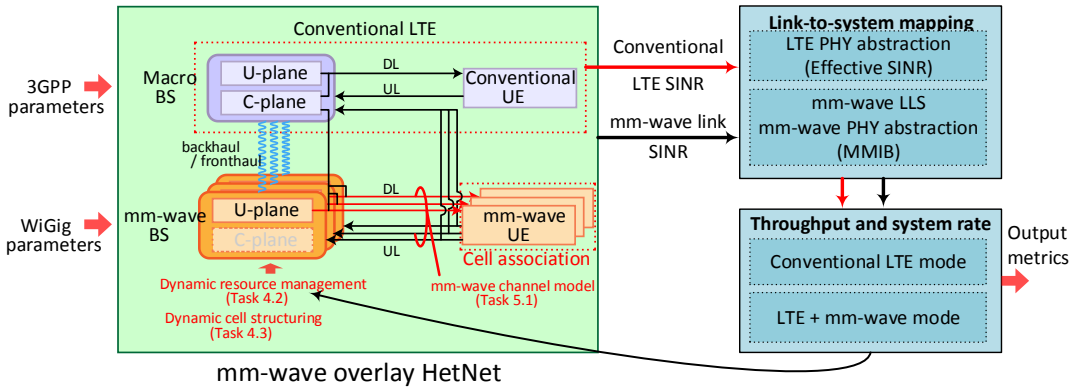

Figure 1.1-1 Overall simulator architecture

Figure 1.1-1 shows the overall system level simulator architecture. It is separated into a conventional LTE system and the novel mm-wave small cells system for both uplink (UL) and downlink (DL). In this deliverable, only DL is presented. For the LTE system, it contains macro cells where one macro cell is responsible for the control (C)-plane of all base stations within the cell. LTE small cells with user (U)-plane are also implemented as a comparison of the proposed mm-wave overlay HetNet with a LTE HetNet. LTE system's parameters are adopted from 3GPP. For the novel mm-wave small cells, only the mm-wave U-plane access links with UE got implemented for the time being. The mm-wave small cells' C-plane is an open issue to be discussed in WP3 and will be implemented in the future if necessary. The access link parameters are adopted from both IEEE 802.11ad (WiGig) as well as from parameters based on MiWEBA measurement results. Especially, the new channel model for the mm-wave access links is input from D5.1. The mm-wave small cells are assumed to be perfectly connected to the C-plane of the LTE network (C-RAN) by backhaul or front haul. The backhaul/ front haul parameters (e.g. for CPRI) are not part of this deliverable. With the above architecture, UEs' C-plane are only connected to the macro LTE, while UEs' U-plane can connect to both systems (LTE macro or small cells and the novel mm-wave small cells).

As all UEs are commonly connected to the macro BS's C-plane at C-RAN, the architecture allows dynamic resource management, developed in T4.2, such as optimal user association and scheduling, time/frequency/space resource assignment; and also dynamic cell structuring of mm-wave small cells (developed in T4.3), where BSs cooperate at PHY layer to transmit to their serving UEs.

To evaluate the real system level performance of LTE with mm-wave overlay HetNet, for each time slot of the user scheduler, the simulator calculates the instantaneous SINRs of UEs for both conventional LTE and mm-wave modes. The SINR metrics then recalculated into the modulation-coding schemes (MCSs) for both PHYs and corresponding to that schemes packet error rate (PER) metrics, by using appropriate LTE or mm-wave PHY abstraction methodologies (see Section 2), thus providing the effective user throughput for each PHY. This information may be further used for Dynamic resource management (see Figure 1.1-1). Long-term performances, e.g. average throughputs, are calculated at the end of the scheduler by

adapting to a time/frequency varying channels implemented for each UE in the System Level Simulator

2 Link level simulator

2.1 Link level simulator for 2GHz and 3.5GHz LTE

The link-level simulator (LLS) for LTE evaluates link-level performance, such as bit error rate (BER) and/or block error rate (BLER), on a given link channel condition. The evaluation results of LLS are used for PHY abstraction on the system level simulator (SLS) by means of link-to-system mapping methods, e.g. Exponential effective SINR Mapping [1] or Mean Mutual Information per Bit (MMIB) mapping detailed on the Section 2.3.

2.1.1 Link level simulator parameters

The physical downlink shared channel (PDSCH) is used to transmit the downlink user-plane data on LTE. Therefore the LLS evaluates the performance of PDSCH based on the 3GPP specification [2] [3] [4]. The channel coding, modulation, multiplexing and propagation channel on equivalent low-pass model have been modeled in the LLS. The modeling of time-frequency resource scheduling, link adaptation and time-frequency variant channel are role of SLS. Parameters for the LTE LLS are summarized in Table 2.1.1-1.

TABLE **FEHLER! VERWEISQUELLE KONNTE NICHT GEFUNDEN WERDEN.**-1
LLS PARAMETERS FOR THE LTE

Parameter	Value
Modulation	QPSK, 16QAM, 64QAM
Multiplexing	OFDM (15kHz sub-carrier spacing, 4.7 or 5.2μs cyclic prefix)
Coding	LTE Turbo code (base coding rate R=1/3, K=4, QPP interleave)
Transmission bandwidth	25 resource blocks (4.5MHz)
Channel model	AWGN

The LTE supports scalable bandwidth allocation and flexible channel coding rate. The channel coding scheme of the LTE is implemented as a combination of a fixed r=1/3 turbo encoder and a rate matching process [5]. By means of rate matching, any arbitrary code rate can be achieved from a fixed-rate mother code [6]. The accurate code rate of a code block is calculated by dividing the size of the transport block (TB), which is a block of information bits to carry a MAC PDU, by the number of allocated time-frequency resources elements (REs) and the modulation order.

2.1.2 Evaluation results

The LLS is performed with typical coding rates that are defined on CQI table [3]. Though the mother code rate r=1/3 is not listed in the CQI table, the performance is necessary for mapping BLER performance with Incremental Redundancy HARQ on SLS. The transmission bandwidth is set to 25 resource blocks (4.5MHz). Table 2.1.2-1 shows the list of evaluated modulation and coding schemes.

Table 2.1.2-1: The evaluated modulation and coding schemes

CQI index	Modulation	Code rate	Spectral efficiency [bps/Hz]
1	QPSK	78/1024	0.1523
2	QPSK	120/1024	0.2344
3	QPSK	193/1024	0.3770
4	QPSK	308/1024	0.6016
N/A	QPSK	1/3	0.6667
5	QPSK	449/1024	0.8770
6	QPSK	602/1024	1.1758
N/A	16QAM	1/3	1.3333
7	16QAM	378/1024	1.4766
8	16QAM	490/1024	1.9141
9	16QAM	616/1024	2.4063
N/A	64QAM	1/3	2.0000
10	64QAM	466/1024	2.7305
11	64QAM	567/1024	3.3223
12	64QAM	666/1024	3.9023
13	64QAM	772/1024	4.5234
14	64QAM	873/1024	5.1152
15	64QAM	948/1024	5.5547

The BLER performances evaluated by the LLS are shown on Figure 2.1-1.

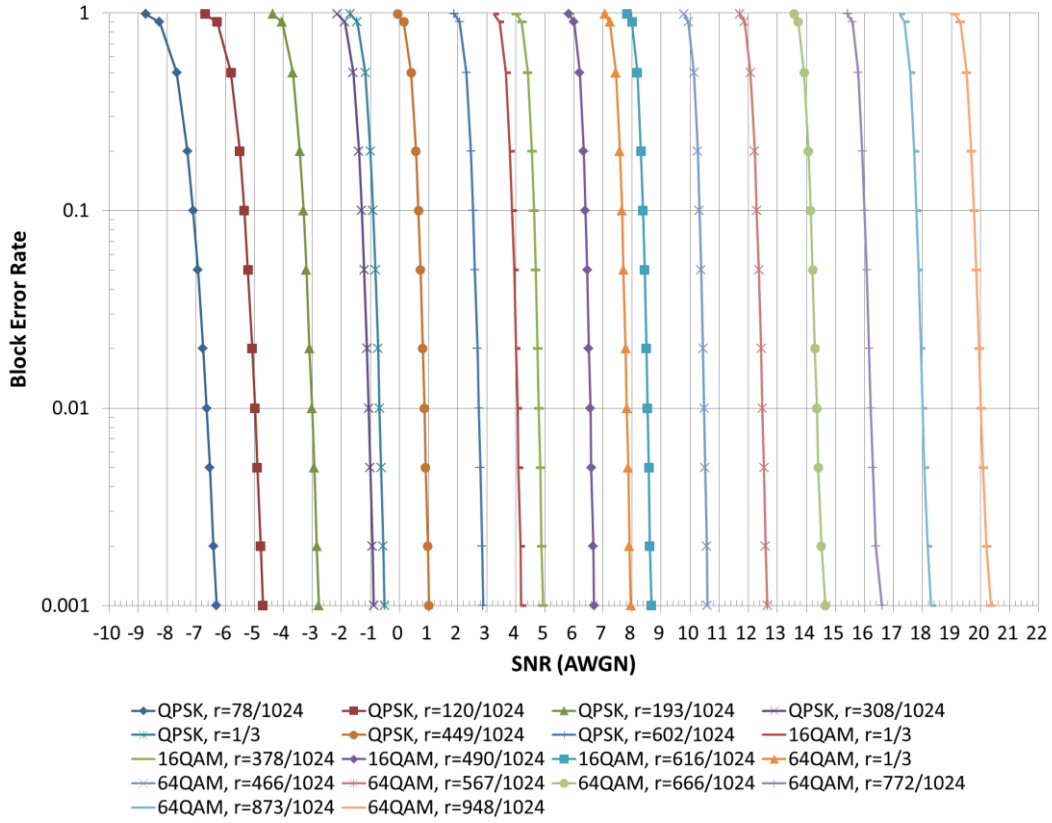

Figure 2.1-1 LTE link level BLER performance on AWGN channel

The link adaptation function on scheduler selects a MCS to get the highest spectrum efficiency while satisfying target BLER. In typical usage with Hybrid-ARQ supported system, target BLER is set to 10–20%. Figure 2.1-1 shows that the LTE supports wide range of MCSs to utilize wide range of SNR from -7dB to 19dB with BLER=10%.

2.2 Link level simulator for 60GHz WiGig

The Link Level Simulation (LLS) platform was designed to support modelling of Physical (PHY) layer defined in the IEEE 802.11ad standard. It can be used as a standalone tool to verify link level behaviour and evaluate demodulator and decoder performance, estimate Radio Frequency (RF) chain imperfections, comply with Error Vector Magnitude (EVM) or Spectral Mask (SM) tests. This makes LLS an essential tool for PHY layer performance verification and gets insight into algorithmic part of the transceiver design. The LLS tool can be used as a part of the System Level Simulation (SLS) platform applying to estimate overall system performance and demonstrate simultaneous work of several hundreds or thousands users for the target scenario. In that case the LLS platform is considered as a building block which simulates a link between the pair of devices.

The approach running LLS for every link in order to evaluate system level performance is not feasible for the great number of users due to computational complexity and time consumption issue. Each LLS run would need decoding of the packets which is a hard part of its signal processing pipeline and would require significant time and computational resources. To overcome this issue PHY

abstraction model predicting Bit Error Rate (BER) or Packet Error Rate (PER) encoded performance without modelling of the entire LLS data flow is introduced. In that approach LLS is used to produce the basic set of the average BER versus Signal to Noise Ratio (SNR) curves for the considered modulations and encoding rates in the frequency flat channel with Additive White Gaussian Noise (AWGN). These curves are used as an input to the PHY abstraction model in order to get instantaneous BER/PER performance estimation for every link considered in the SLS. This PHY abstraction model is developed for the desired channel and depends on the considered channel type.

In this section the LLS platform implementing the PHY abstraction model, implementing IEEE 802.11ad standard, based on the Mean Mutual Information per Bit (MMIB) metric is considered firstly and then the SLS platform description concludes the section.

2.2.1 IEEE 802.11ad PHY Layer Overview

The IEEE 802.11ad standard supports Directive Multi Gigabit (DMG) PHY layer with three modulation methods, namely control modulation which supports differential BPSK (DBPSK), Single Carrier (SC) and Orthogonal Frequency Division Multiplexing (OFDM) modulation.

Table 2.2.1-1 gives a summary of the modulations defined in the IEEE 802.11ad standard and corresponding data rates.

Table 2.2.1-1: Summary of modulation types used in IEEE 802.11ad standard

Modulation type	Modulation Coding Scheme (MCS) index	Data rates, [Mbps]
Control modulation	0	27.5
Single Carrier (SC)	1 - 12	385.0 – 4620.0
OFDM	13 - 24	693.0 - 6756.75
SC low power	25 - 31	626.0 – 2503.0

The control DBPSK, SC (except SC low power) and OFDM modulations support common Low Density Parity Check (LDPC) code with rates ½, 5/8, ¾ and 13/16. This code is designed based on the 4 parity check matrices defining the rate and allows Belief Propagation (BP) and Layered Belief Propagation (LBP) decoding.

The control PHY bit stream is encoded using effective LDPC code rate less than or equal to ½ generated from the LDPC code with rate ¾ applying shortening procedure.

The SC PHY uses π/2-BPSK, π/2-QPSK, and π/2-16QAM modulations. Table 2.2.1-2 below gives a summary of Modulation and Coding Scheme (MCS) indexes

corresponding to particular modulation and encoding rate and resulting data rate in case of SC PHY. SC PHY supports the data rates up to 4620.0 Mbps.

Table 1.2.1-2: Modulation and Coding Schemes (MCSs) defined for SC PHY (except SC low power mode)

MCS index	Modulation	Code rate	Data rate, [Mbps]
1	π/2-BPSK	½ (repetition 2x is used)	385.0
2	π/2-BPSK	1/2	770.0
3	π/2-BPSK	5/8	962.5
4	π/2-BPSK	3/4	1155.0
5	π/2-BPSK	13/16	1251.25
6	π/2-QPSK	1/2	1540.0
7	π/2-QPSK	5/8	1925.0
8	π/2-QPSK	3/4	2310.0
9	π/2-QPSK	13/16	2502.5
10	π/2-16QAM	1/2	3080.0
11	π/2-16QAM	5/8	3850.0
12	π/2-16QAM	3/4	4620.0

The OFDM PHY uses SQPSK (Spread QPSK), QPSK, 16QAM and 64QAM modulations. Table 2.1.2-3 below gives a summary of MCS indexes corresponding to particular modulation and encoding rate and resulting data rate in case of OFDM PHY. OFDM PHY introduces 64QAM modulation and therefore supports data rates extension up to 6756.75 Mbps.

Table 2.1.2-3: Modulation and Coding Schemes (MCSs) defined for OFDM PHY

MCS index	Modulation	Code rate	Data rate, [Mbps]
13	SQPSK	1/2	693.0
14	SQPSK	5/8	866.25
15	QPSK	1/2	1386.0
16	QPSK	5/8	1732.5
17	QPSK	3/4	2079.0
18	16-QAM	1/2	2772.0
19	16-QAM	5/8	3465.0
20	16-QAM	3/4	4158.0
21	16-QAM	13/16	4504.5
22	64-QAM	5/8	5197.5
23	64-QAM	3/4	6237.0
24	64-QAM	13/16	6756.75

The MCSs 0 – 4 are mandatory for implementation in all IEEE 802.11ad eligible devices. All other transmission modes are optional.

The SC low power PHY is a special mode that can provide low processing power requirements for IEEE 802.11ad transceivers. It does not support LDPC encoding, but rather provides less complicated Reed Solomon (RS) and binary block codes. Therefore SC low power mode does not allow soft input decoder which significantly reduces the performance of Forward Error Correction (FEC) scheme. SC low power PHY is optional and not supported by the majority of the silicon vendors. The developed LLS platform supports control DBPSK, SC and OFDM PHYs (MCS 0 – 24) and does not support SC low power PHY (MCS 25 – 31).

2.2.1.1 Frame Structure

All modulation methods defined in the IEEE 802.11ad standard use a general frame structure shown in Fig. 2.2.1.1-1 and composed of the preamble, header, payload data part and optional Automatic Gain Control (AGC) and TRN-T/R subfields.

Figure 2.2.1.1-1: General frame structure defined in IEEE 802.11ad standard.

The preamble is used for packet detection, AGC, Carrier Frequency Offset (CFO) estimation, synchronization, noise power estimation, indication of the frame type and channel estimation. It is composed of the Short Training Field (STF) and Channel Estimation Field (CEF) as shown in Fig. 2.2.1.1-2. The STF and CEF fields are different for different modulation methods and will be considered later.

Figure 2.2.1.1-2: Preamble structure defined in IEEE 802.11ad standard.

The preamble is followed by the header which consists of several fields that define the parameters of the PHY Service Data Unit (PSDU) transmission provided by Medium Access Control (MAC) layer. These parameters may include scrambler initialization seed, MCS index, length of the transmitted PSDU, Header Check Sequence (HCS) and other fields. The header type depends on the modulation method and the detailed description of its structure can be found in [7].

The payload data contains PSDU transferred to PHY from MAC layer. The AGC and TRN-T/R subfields are optional and the description of their structure can be found in [7].

The developed LLS platform supports preamble, header and payload data transmission and does not support AGC and TRN-T/R optional subfields.

2.2.1.2 Control Modulation

The control PHY modulation is defined at the 1.76 GHz sample rate. So the duration of 1 sample is equal to ~0.57 ns.

The preamble of control PHY is composed of complementary Golay sequences Ga_{128} and Gb_{128} of length 128 samples defined in [7]. The Short Training Field (STF) of the preamble consists of 48 repetitions of Golay sequence Gb_{128} followed by a single $-Gb_{128}$ sequence with inverse sign and then a single $-Ga_{128}$ sequence. The duration of STF is equal to ~3.6 µs. Figure 2.2.1.2-1 below shows STF field for control PHY.

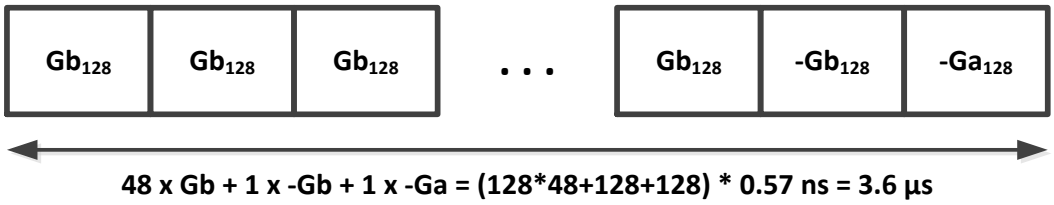

Figure 2.2.1.2-1: Short Training Field (STF) for control PHY defined in IEEE 802.11ad standard.

The Golay Ga_{128} and Gb_{128} are real sequences composed of ±1 similar to BPSK modulation. In order to prevent phase flip by π, the phase of consequent samples in Ga_{128}/Gb_{128} is rotated by π/2. Hence Ga_{128}/Gb_{128} sequences become complex and the phase difference between adjacent sample does not exceed π/2.

The Channel Estimation Field (CEF) of preamble consists of 9 $\pm Ga_{128}/\pm Gb_{128}$ sequences as shown in Fig. 2.2.1.2-2. The duration of CEF is equal to ~0.65 µs. The first 4 $\pm Ga_{128}/\pm Gb_{128}$ sequences are united into Gu_{512} and the second 4 $\pm Ga_{128}/\pm Gb_{128}$ sequences are united into Gv_{512} sequence.

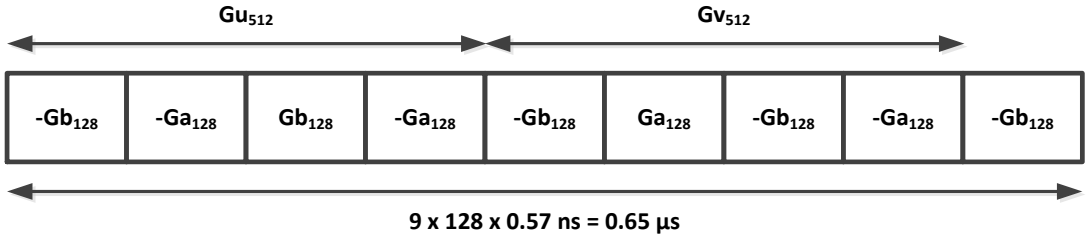

Figure 2.2.1.2-2: Channel Estimation Field (CEF) for control PHY defined in IEEE 802.11ad standard.

Similar to STF the phases of consequent samples of CEF are rotated by π/2.

The header and payload data parts of the control PHY frame is encoded with rate ½ generated from the LDPC code with rate ¾ applying shortening procedure. The scrambled and coded bit stream is converted into constellation points using DBPSK modulation. Then the DBPSK constellation points are spread using the Golay sequence Ga_{32} of length 32 samples which is defined in [7]. Similar to STF and CEF the phases of the consequent samples of the resulting ±1 sequence are rotated by π/2.

2.2.1.3 Single Carrier Modulation

The SC PHY modulation is defined at the 1.76 GHz sample rate and sample duration is equal to ~0.57 ns.

The STF for SC PHY is composed of 16 repetitions of Golay sequence Ga_{128} followed by a single sequence $-Ga_{128}$ with inverse sign. The duration of STF is equal to ~1.24 µs. Figure 2.2.1.3-1 below shows STF field for SC PHY.

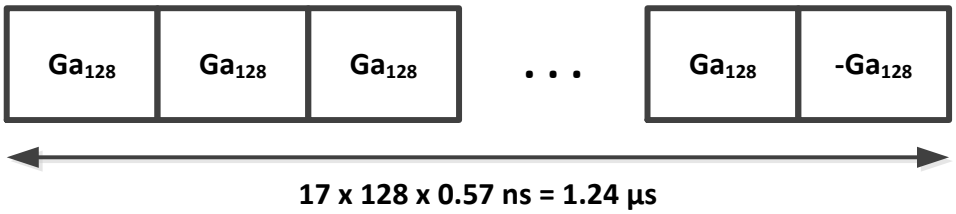

Figure 2.2.1.3-1: Short Training Field (STF) for SC PHY defined in IEEE 802.11ad standard.

Similar to STF of control PHY the phases of consequent samples of STF SC PHY are rotated by π/2. The CEF for SC PHY is the same as for the control PHY shown in Fig. 2.2.1.2-2.

The SC PHY uses LDPC code with rates ½, 5/8, ¾, and 13/16 and π/2-BPSK, π/2-QPSK, and π/2-16QAM modulations. The encoded and modulated symbols stream is divided into blocks of length 448 samples. Note that bit padding is applied in order to get the integer number of blocks to be transmitted. Each block of 448 symbols is prepended with Guard Interval (GI) of length 64 samples. The duration of SC block is equal to ~0.29 µs. The SC PHY blocks structure is shown in Fig. 2.2.1.3-2 below.

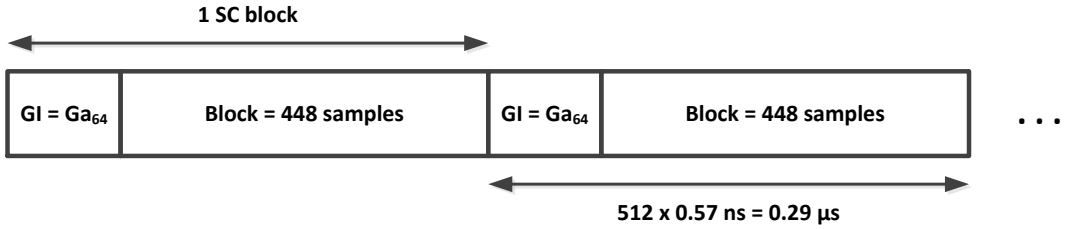

Figure 2.2.1.3-2: SC PHY blocks structure defined in IEEE 802.11ad standard.

The GI is defined as Ga_{64} Golay sequence of length 64 samples defined in [7]. Note that phases of consequent samples of Ga_{64} are rotated by π/2.

Summary of SC signal parameters specified in the IEEE 802.11ad standard is presented in Table 2.2.1.3-1.

Table 2.2.1.3-1: Summary of SC signal parameters defined in IEEE 802.11ad standard

Parameter	Value
Number of data symbols in the block	448

Sampling frequency	1.76 GHz
Guard Interval size and duration	64 samples * 0.57 ns = 36.3 ns
SC block duration	0.29 µs

The encoding procedure for the header is defined in such a way that header is mapped into 2 SC blocks. For header transmission π/2-BPSK modulation is used.

The resulting SC PHY frame taken at 1.76 GHz sample rate is processed by the digital shape filter which is not defined in the IEEE 802.11ad standard and is vendor specific. The choice of shape filter is implementation specific as long as Error Vector Magnitude (EVM) and transmit spectral mask requirements are met.

2.2.1.4 OFDM Modulation

The OFDM PHY modulation is defined at the 2.64 GHz = 1.5 x 1.76 GHz sample rate which is 1.5 times greater comparing to the SC sample rate. The corresponding sample duration is equal to ~0.38 ns.

The preamble defined for the OFDM PHY is similar to the SC PHY. The STF for OFDM is exactly the same as for SC PHY shown in Fig. 2.2.1.3-1. The CEF for OFDM PHY is shown in Fig. 2.2.1.4-1. The only difference from control PHY and SC PHY shown in Fig. 2.2.1.2-2 is the ordering of Gu_{512} and Gv_{512} sequences. For the OFDM PHY they follow each other in reverse order.

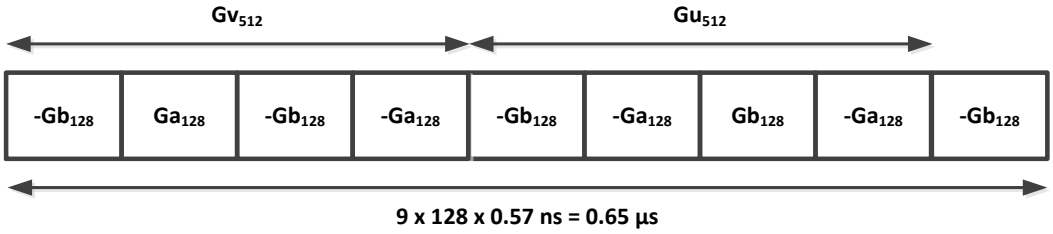

Figure 2.2.1.4-1: Channel Estimation Field (CEF) for OFDM PHY defined in IEEE 802.11ad standard

Note that preamble is defined at the 1.76 GHz sample rate, but the header and payload data are sampled at 2.64 GHz. In order to get preamble at 2.64 GHz sample rate the special resampling procedure is defined in the standard. The steps of resampling procedure are shown in Fig. 2.2.1.4-2 (a). Figure 2.2.1.4-2 (b) shows resampling filter impulse response of length 71 samples defined in the standard.

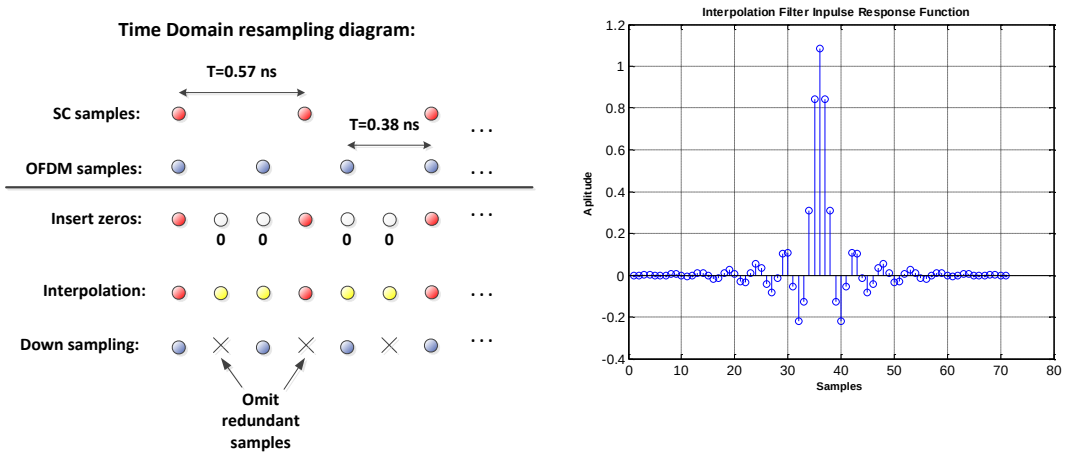

(a) Resampling procedure **(b) Resampling filter impulse response**

Figure 2.2.1.4-2: Illustration of preamble resampling procedure defined for OFDM PHY in IEEE 802.11ad standard.

The resampling procedure includes the following steps:

1. **Insert zeroes:** SC sampling rate is increased 3x times adding 2 zeroes after each SC sample;
2. **Interpolation:** 3 x 1.76 GHz = 5.28 GHz signal is convolved with resampling filter impulse response shown in Fig. 2.2.1.4-2 (b), note that filter is defined at the same (5.28 GHz) sample rate;
3. **Down sampling:** SC sampling rate decreased 2x times omitting every second sample;

After resampling the resulting preamble waveform is represented at the 2.64 GHz sample rate.

In contrast to SC PHY the mapping to OFDM symbols is done in frequency domain. There are in total 512 subcarriers including 336 data subcarriers, 16 pilots, 3 zero DC subcarriers, and 79 zeroes for the left guard and 78 for the right guard bands. Figure 2.2.1.4-3 below shows subcarriers mapping in OFDM signal.

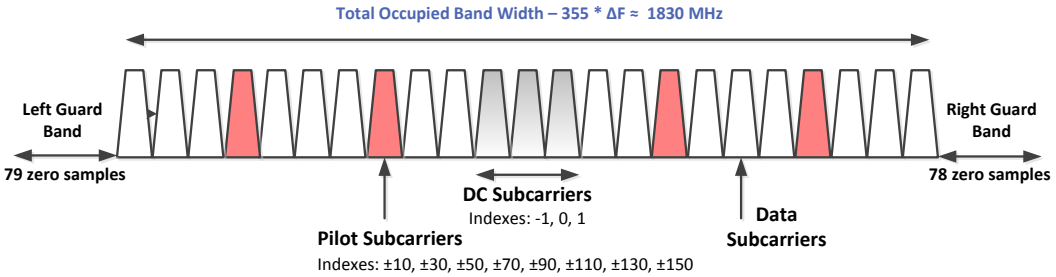

Figure 2.2.1.4-3: Illustration of OFDM subcarriers mapping defined in IEEE 802.11ad standard.

The OFDM PHY uses LDPC code with rates ½, 5/8, ¾, and 13/16 and SQPSK (Spread QPSK), QPSK, 16QAM and 64QAM modulations. The encoded and modulated symbols stream is divided into blocks of length 336. Note that bit padding is applied in order to get the integer number of blocks to be transmitted. Each block of 336 symbols is mapped into OFDM symbol.

The 16 pilots are transmitted in every OFDM symbol and regularly spaced in frequency domain with subcarrier indexes {±10, ±30, ±50, ±70, ±90, ±110, ±130, ±150}. The initial pilot sequence is predefined and composed of ±1, but the sign of all pilots can be inverted in accordance with bit value coming from scrambler. The initial scrambler seed is equal to all ones sequence.

After mapping completion the Inverse Fast Fourier Transform (IFFT) is applied in order to get OFDM symbol in time domain. Each OFDM symbol of length 512 samples is prepended with Cyclic Prefix (CP) of length 128 samples. The CP taken from the tail of the symbol is cyclically extended into beginning of the OFDM symbol as shown in Fig. 2.2.1.4-4. So, the resulting OFDM symbol length is equal to 640 samples.

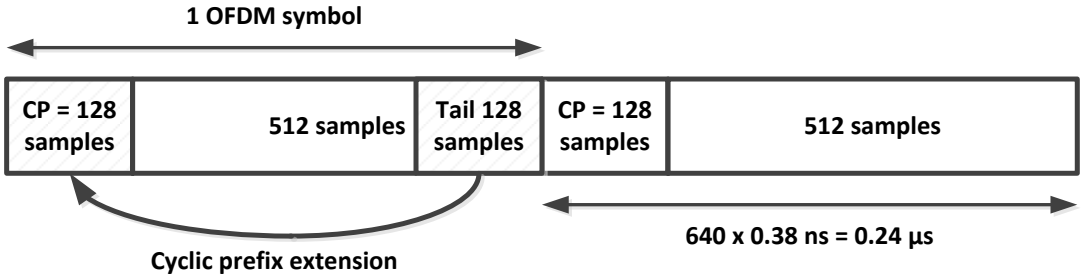

Figure 2.2.1.4-4: OFDM PHY symbols structure defined in IEEE 802.11ad standard.

Summary of OFDM signal parameters specified in the IEEE 802.11ad standard is presented in Table 2.2.1.4-1.

Table 2.2.1.4-1: Summary of OFDM signal parameters defined in IEEE 802.11ad standard

Parameter	Value
Number of data subcarriers	336
Number of pilots	16
Number of DCs	3
Sampling frequency	2.64 GHz
Subcarrier spacing	2640/512 = 5.156 MHz
Cyclic prefix size and duration	128 samples * 0.38 ns = 48.4 ns

FFT/IFFT size and duration	512 samples * 0.38 ns = 0.194 µs
OFDM symbol duration	0.24 µs

The encoding procedure for the header is defined in such a way that header is mapped into 1 OFDM symbol. For header transmission QPSK modulation is used.

The phase transitions between consequent OFDM symbols taken at 2.64 GHz sample rate can be smoothed by application of windowing function. The choice of windowing function is implementation specific as long as EVM and transmit spectral mask requirements are met.

2.2.1.5 LDPC Code

Four Low Density Parity Check (LDPC) codes are defined by the four parity matrices for each encoding rate ½, 5/8, ¾ and 13/16. All encoding rates have common codeword size of 672 bits, but different amount of parity size.

Each parity matrix is composed of square bit sub matrices of size Z. The square sub matrix of size Z is either right cyclic permutation of the identity matrix or null matrix with all zero elements.

The examples of bit permutation matrix $\mathbf{P_i}$ for Z = 4 and right cyclic shifts i=1 and 3 are shown in Fig. 2.2.1.5-1 below.

$\mathbf{P_1} =$

0	1	0	0
0	0	1	0
0	0	0	1
1	0	0	0

$\mathbf{P_3} =$

0	0	0	1
1	0	0	0
0	1	0	0
0	0	1	0

Figure 2.2.1.5-1: Examples of bit permutation matrices P_i for i = 1 and 3.

An example of parity matrix with encoding rate ½ defined in the IEEE 802.11ad standard is shown in Fig. 2.2.1.5-2.

40	-1	38	-1	13	-1	5	-1	18	-1	-1	-1	-1	-1	-1	-1
34	-1	35	-1	27	-1	-1	30	2	1	-1	-1	-1	-1	-1	-1
-1	36	-1	31	-1	7	-1	34	-1	10	41	-1	-1	-1	-1	-1
-1	27	-1	18	-1	12	20	-1	-1	-1	15	6	-1	-1	-1	-1
35	-1	41	-1	40	-1	39	-1	28	-1	-1	3	28	-1	-1	-1
29	-1	0	-1	-1	22	-1	4	-1	28	-1	27	-1	23	-1	-1
-1	31	-1	23	-1	21	-1	20	-1	-1	12	-1	-1	0	13	-1
-1	22	-1	34	31	-1	14	-1	4	-1	-1	-1	13	-1	22	24

Figure 2.2.1.5-2: Example of parity check matrix for rate ½ defined in the IEEE 802.11ad standard.

The elements of this matrix represent right cyclic shift values defined for the square matrix of size Z = 42, -1 value defines null matrix entity. Substituting identity matrices of size 42 bits with specified cyclic shift into matrix shown in Fig. 2.2.1.5-2 one can get a bit matrix shown in Fig. 2.2.1.5-3.

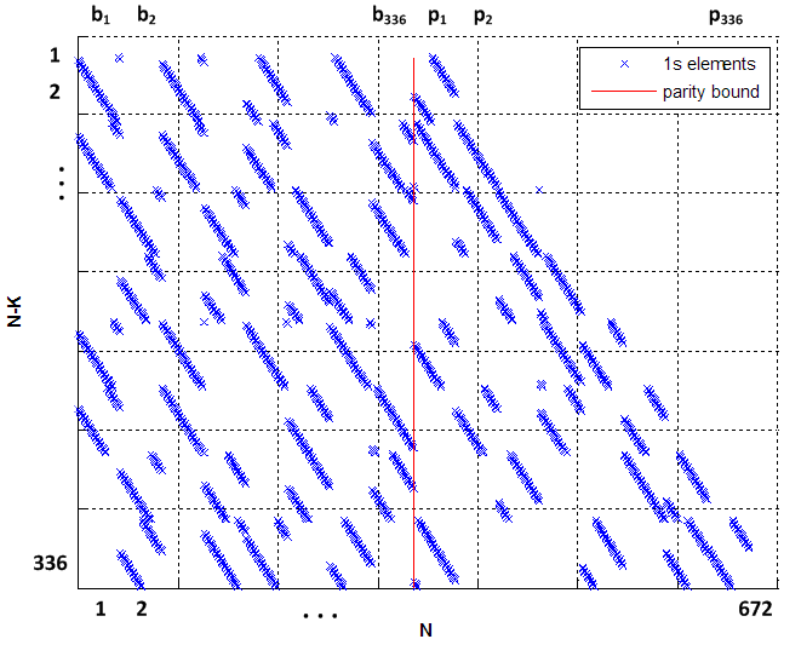

Figure 2.2.1.5-3: Example of parity check matrix for rate ½ with substituted cyclically shifted identity matrices.

The columns dimension of the parity matrix is equal to 672 bits which is a codeword size. The rows dimension is equal to the amount of parity and for the matrix with rate ½ it is 336 bits.

All other matrices corresponding to the encoding rates 5/8, ¾, and 13/16 are defined in a similar way and can be found in the standard [7].

2.2.1.6 Beam forming

The Directive Multi Gigabit (DMG) PHY supports transmission using steerable directive antennas which are usually phased antenna arrays and beam forming protocol in order to setup directional link. The IEEE 802.11ad standard basically defines two types (or phases) of beam forming protocol:

1. Sector Sweep (SS) protocol;
2. Beam Refinement Protocol (BRP);

The Sector Sweep (SS) protocol is implemented using control PHY frames exchange. The SS beam forming can be realized using Transmit Sector Sweep (TXSS) and/or Receive Sector Sweep (RXSS) protocol. Most of IEEE 802.11ad chipmakers implement TXSS protocol as a basic one to set up directional beam forming link and consider RXSS as an optional part. Therefore TXSS protocol is further considered in details and description of RXSS can be found in [7].

The TXSS protocol includes 4 phases:

1. Initiator Sector Sweep (ISS) to train the initiator link;
2. Responder Sector Sweep (RSS) to train the responder link;
3. Sector Sweep (SSW) feedback;
4. SSW acknowledgement (ACK);

These 4 phases are shown in Fig. 2.2.1.6-1 below.

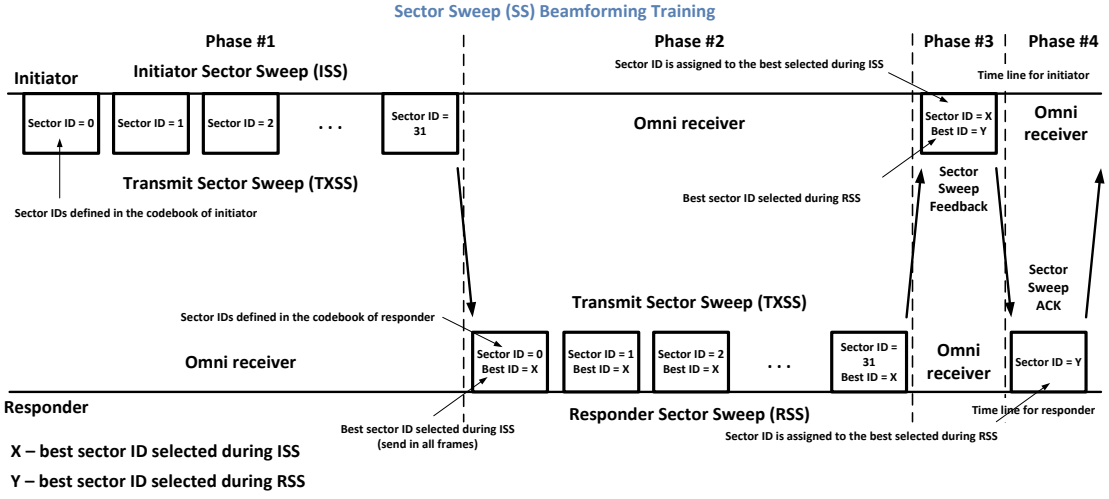

Figure 2.2.1.6-1: TXSS beam forming protocol illustration.

The horizontal parallel lines in the picture show timelines for initiator and responder. In phase 1 the initiator starts performing Initiator Sector Sweep (ISS) and

transmitting packets using control PHY MCS 0 with antenna weights corresponding to different Sector IDs defined in the codebook. The codebook is not defined in the standard and is vendor specific.

The antenna settings are applied for the whole packet transmission. An example in Fig. 2.2.1.6-1 assumes that the codebook is composed of 32 Sectors with Sector ID = 0, 1,…,31. During ISS the responder receives packets using omni antenna pattern. After completion of ISS, the responder defines the best Sector ID = X for initiator based on some criterion. Figure 2.2.1.6-2 (a) shows antenna patterns for ISS beam forming in phase 1.

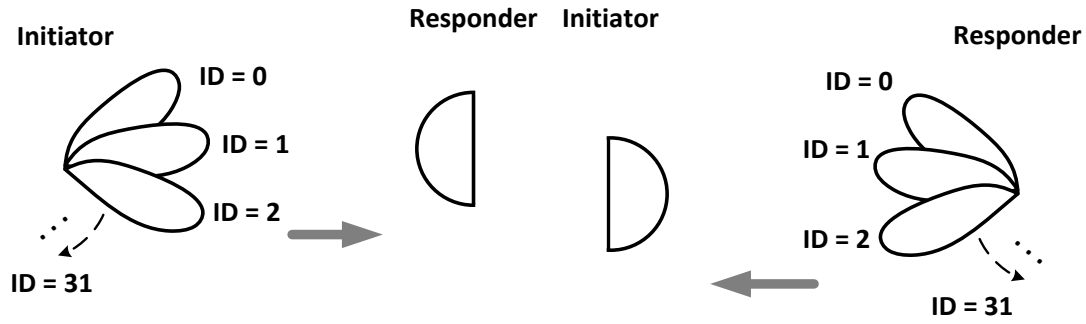

(a) Phase 1 - Initiator Sector Sweep (ISS) **(b) Phase 2 - Responder Sector Sweep (RSS)**

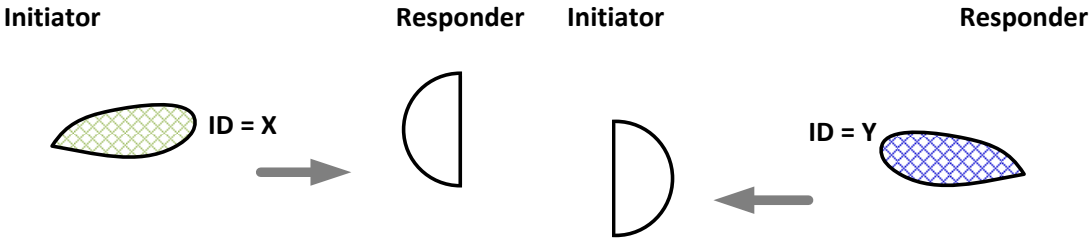

(c) Phase 3 – Sector Sweep (SSW) feedback **(d) Phase 4 – Acknowledgement (ACK)**

Figure 2.2.1.6-2: Antenna patterns in TXSS beam forming protocol.

In phase 2 the responder starts performing Responder Sector Sweep (RSS) and transmitting packets using control PHY MCS 0 with antenna weights corresponding to different Sector IDs defined in the codebook. During RSS the initiator receives packets using omni antenna pattern. Note that all packets sending by responder contain the best Sector ID = X selected during ISS. After completion of RSS, the initiator defines the best Sector ID = Y for responder based on the same criterion. Figure 2.2.1.6-2 (b) shows antenna patterns for RSS beam forming in phase 2.

In phase 3 the initiator transmits single Sector Sweep (SSW) feedback frame with the information about the best Sector ID = Y for responder. The initiator makes

transmission applying antenna configuration for the Sector with ID = X. The responder receives the feedback packet using omni antenna pattern. Figure 2.2.1.6-2 (c) shows antenna patterns for SSW feedback in phase 3.

In phase 4 the responder confirms the selected Sector ID = Y by sending single acknowledgement (ACK) frame. The initiator uses omni antenna pattern to receive ACK frame. Figure 2.2.1.6-2 (d) shows antenna patterns for ACK in phase 4.

After these 4 phases the directional PHY transmission is allowed applying antennas settings with Sector ID = X for initiator and ID = Y for responder.

The SS beam forming protocol does not use exhaustive search algorithm, but rather uses omni directional antenna at one end of the link. This introduces additional requirements for the performance of control PHY. The control PHY defined in IEEE 802.11ad standard allows robust frames transmission for Signal to Noise Ratio (SNR) up to -14.0 dB.

After completion of SS part of beam forming protocol data transmission is allowed. For the directive data transmission SC or OFDM PHY can be used.

The Beam Refinement Protocol (BRP) is an optional feature and is done after SS beam forming completion using optional TRN-T/R subfields appended to the frame. The purpose of the BRP phase is to enable further iterative refinement of the antenna weights. In contrast to the SS protocol, BRP can be implemented using control PHY, SC or OFDM frames exchange. The detailed description of the BRP phase of the beam forming protocol can be found in [7].

Finally note that beam forming protocol is implemented in the SLS platform and the LLS platform uses the provided channel impulse response for the desired antenna weights after completion of the beam forming protocol.

2.2.2 Link Level Simulation Platform

The Link Level Simulation (LLS) platform supports control PHY (MCS = 0), SC (MCS = 1 – 12) and OFDM (MCS = 13 - 24) modulation methods. It supports transmission and reception of IEEE 802.11ad frames composed of preamble, header, and payload data part.

The LLS platform is written using C++ language and uses class paradigm to design building blocks. The main class implementing LLS platform is called `Sta` (from "Station"). It has three public functions `Sta->config(txVector)`, `Sta->transmit(psdu, waveform)`, and `Sta->receive(waveform, psdu, StaAcq, rxVector)` which make LLS platform configuration, waveform transmission and waveform reception accordingly. Figure 2.2.2-1 shows high level block diagram of LLS platform and corresponding `Sta` class functions.

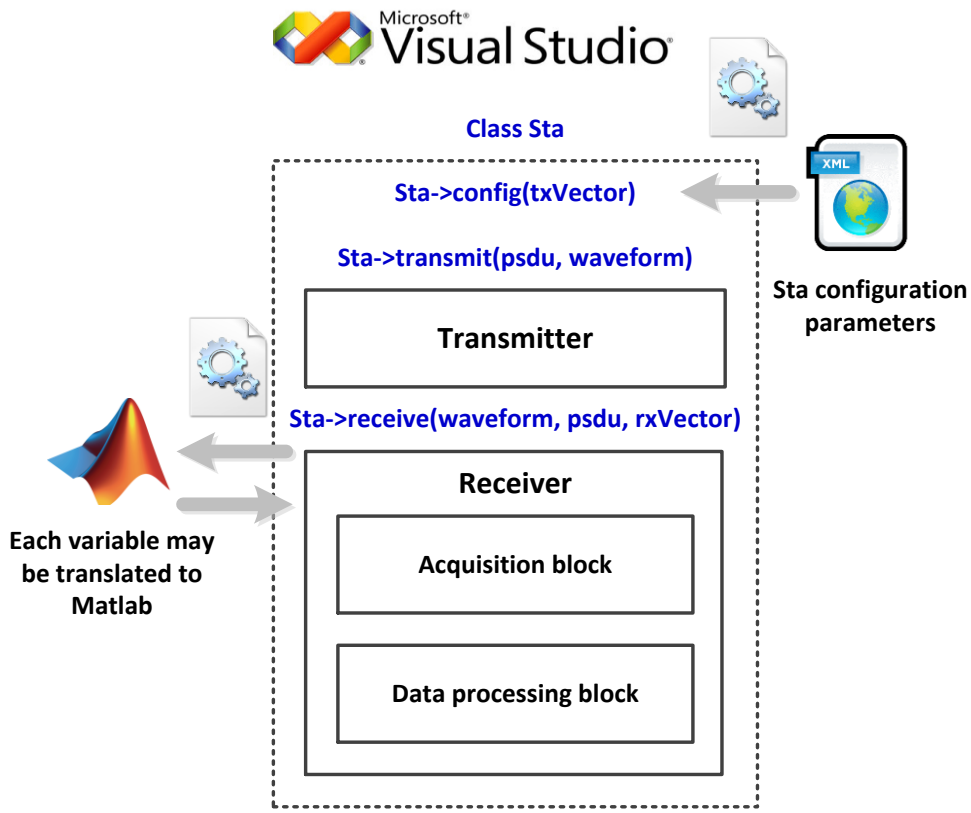

Figure 2.2.2-1: High level block diagram of LLS platform.

The configuration function `Sta->config(txVector)` assigns all parameters required for frame transmission defined in the `txVector` structure. The `txVector` structure can be initialized from the XML configuration file using configuration builder routine. If LLS is embedded into SLS platform the `txVector` can be transferred directly from the SLS. Table 2.2.2-1 gives a summary of `txVector` fields defined for the `Sta`.

Table 2.2.2-1: txVector structure fields description

Structure field	**Short description / possible values**
`m_Mcs`	Field indicates the Modulation and Coding Scheme (MCS) for PSDU transmission / 0 – 24
`m_PsduLength`	PSDU length in bytes / 14–1023 for control PHY, 1 – 262143 for SC/OFDM PHY, 0 if PSDU is not transmitted;
`m_ScrSeed`	Scrambler initial state (seed) / 0 - 127

m_DtpType	STATIC or DYNAMIC tone pairing (OFDM specific parameter) / 0 or 1 (see IEEE 802.11ad std. for details, [8])
m_GroupPairIndex	DYNAMIC tone pairing indexes (OFDM specific parameter) / 1 – 42 (see IEEE 802.11ad std. for details, [8])

To simplify debugging process and for the sake of data visualization Visual Studio (VS) has interface to the Matlab environment. The special routine `sendToMatlab()` allows to translate any variable or array from VS to Matlab. The routine `getFromMatlab()` translates any variable from the Matlab environment to VS.

The function `Sta->transmit(psdu, waveform)` can generate baseband waveform for control PHY, SC or OFDM modulation. For control PHY or SC modulation method the baseband waveform can be generated at 1.76 GHz or 2.64 GHz sample rate. For OFDM modulation only 2.64 GHz sample rate is allowed. `Sta->transmit(psdu, waveform)` function can generate up sampling waveform with factors 4x, 8x, and 16x to model an analog signal at the output of Digital to Analog Converter (DAC).

The function `Sta->receive(waveform, psdu, StaAcq, rxVector)` can receive baseband or up sampled waveform and produce estimation of the PSDU. Also it provides `StaAcq` and `rxVector` structures containing metrics for acquisition and decoding performance accordingly.

The receiver is structurally composed of two main blocks (see Fig. 2.2.2-1):

1. Acquisition block which implements packet acquisition algorithms and makes processing of the preamble part of the frame;
2. Data processing block which implements data demodulation and decoding algorithms and makes processing of the header and payload data part of the frame;

The acquisition block provides `StaAcq` structure. The `StaAcq` fields are described in Table 2.2.2-2.

Table 2.2.2-2: StaAcq structure fields description

Structure field	**Short description / possible values**
m_AcqDetFlag	Acquisition detection flag / 1 - on, 0 - off
m_AcqSyncFlag	Acquisition sync flag / 1 - on, 0 - off
m_AcqPhyType	Acquisition PHY type
m_AcqMd	Acquisition Miss Detection rate

m_AcqFa	Acquisition False Alarm rate
m_AcqMs	Acquisition Miss Sync rate
m_AcqFs	Acquisition False Sync rate
m_AcqPhyErr	Acquisition PHY type error rate
m_AcqCfo	Acquisition CFO estimation in ppm
m_AcqPwr	Acquisition noise variance estimation

The data processing block provides rxVector structure. The rxVector fields are described in Table 2.2.2-3.

Table 2.2.2-3: rxVector structure fields description

Structure field	**Short description / possible values**
m_RxHdrFlag	Receiver header flag: 1 - correct HDR, 0 - broken HDR, based on CRC computation
m_RxHer	Receiver Header Error Rate (HER)
m_RxPer	Receiver PSDU Packet Error Rate (PER)
m_RxPsduCwBler	Receiver LDPC code word Block Error Rate (BLER), based on syndrome calculation
m_RxPsduWBler	Receiver LDPC information word BLER, based on direct comparison with transmitter word
m_RxPsduBer	Receiver PSDU Bit Error Rate (BER), based on direct comparison with transmitter PSDU
m_RxIterNum	Receiver LDPC decoder average iterations number per code word
m_RxEvm	Receiver Error Vector Magnitude (EVM) for demodulated PSDU
m_RxPwrN	Receiver additive noise power

In order to estimate packet acquisition and data demodulation and decoding performance two distinct tests were developed. Both tests can be modeled with and without Radio Frequency (RF) chain imperfections such as Carrier Frequency Offset (CFO), Sampling Frequency Offset (SFO), Power Amplifier (PA), and Phase Noise (PN).

2.2.3 Acquisition Test Description

The purpose of acquisition test is to estimate IEEE 802.11ad frame acquisition performance for different channel models using preamble part of the frame. The LLS platform supports frequency flat and IEEE 802.11ad channel models golden set, [9] – [10]:

- Channel 1: Conference Room, omni TX to omni RX, LOS;
- Channel 2: Conference Room, omni TX to directional RX, NLOS;
- Channel 3: Conference Room, directional TX to directional RX, NLOS;
- Channel 4: Living room, omni TX, omni RX, LOS;
- Channel 5: Living room, omni TX, directional RX, NLOS;
- Channel 6: Living room, directional TX, directional RX, NLOS;
- Channel 7: Enterprise Cubicle, near location, omni TX, omni RX, LOS;
- Channel 8: Enterprise Cubicle, far location, omni TX, directional RX, NLOS;
- Channel 9: Enterprise Cubicle, far location, directional TX, directional RX, NLOS;

Acquisition block of the LLS platform has the following functions:

1. Packet detection using Short Training Field (STF);
2. Packet synchronization using STF;
3. PHY type identification using STF and Channel Estimation Field (CEF);
4. Initial Carrier Frequency Offset (CFO) estimation using STF;
5. Channel estimation using CEF;

The packet detection is done using STF of the preamble. For control PHY acquisition block uses repetitions of Gb_{128} sequence (see Fig. 2.2.1.3-1) and for SC or OFDM PHY it uses repetitions of Ga_{128} sequence (see Fig. 2.2.1.4-1). The incoming STF is fed into Golay correlator or Matched Filter (MF) to Ga_{128}/Gb_{128} sequence. Further coherent or non-coherent accumulation of repeated signal can be done. Then it makes binary hypotheses test in order to decide about signal presence at the input of receiver. H_0 hypothesis (null hypothesis) assumes that STF signal has not been received and H_1 hypothesis (alternative hypothesis) assumes that STF signal has been received. The detector calculates decision metric which is a function of the received accumulated signal. It compares decision metric with predefined threshold to decide about H_0/H_1 hypothesis. The detector supports several decision metrics and allows

threshold selection in accordance with Neyman-Pearson theorem or Bayesian criterion.

Figure 2.2.3-1 shows an example of decision metrics distribution for the binary hypotheses test in case of coherent and non-coherent signal accumulation in frequency flat channel with Additive White Gaussian Noise (AWGN). Figure 2.2.3-1 (a) shows distributions for the Signal to Noise Ratio (SNR) at the output of MF per sample equal to SNR = 5.0 dB and Fig. 2.2.3-1 (b) shows corresponding distributions for SNR = 10.0 dB

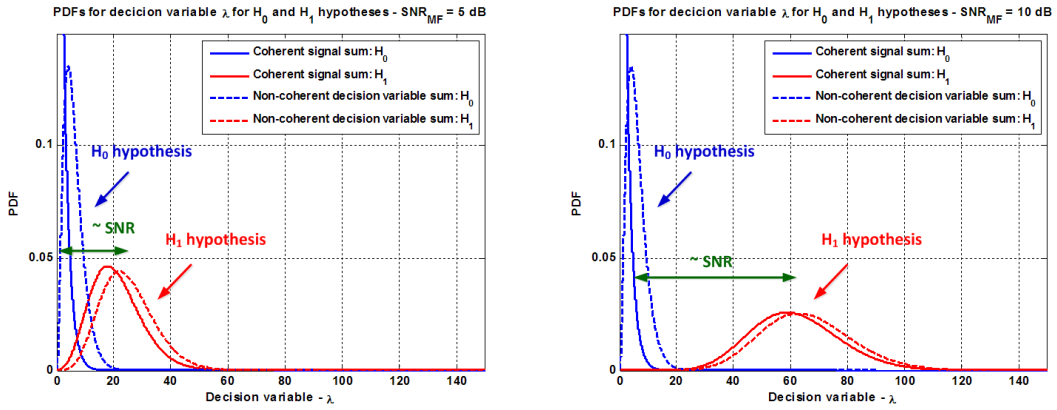

(a) SNR_{MF} = 5.0 dB **(b) SNR_{MF} = 10.0 dB**

Figure 2.2.3-1: Example of decision metrics distribution for binary hypotheses test in case of coherent and non-coherent signal accumulation in frequency flat AWGN channel.

Packet synchronization is done using STF signal at the output of MF and exploits signal sign inversion from Gb_{128} to $-Gb_{128}$ for control PHY (see Fig. 2.2.1.3-1) and Ga_{128} to $-Ga_{128}$ for SC and OFDM (see Fig. 2.2.1.4-1) at the end of the STF field.

Figure 2.2.3-22Figure 2.2.3-2 (a) shows receiver synchronization error rate versus SNR performance without RF chain imperfections and in presence of Phase Noise (PN) (applied at both transmitter and receiver sides) and Carrier Frequency Offset (CFO) equal to 4, 8, 16, and 20 ppm. Figure 2.2.3-2 (b) shows corresponding curves in case of IEEE 802.11ad channel #8. The SNR is introduced at the input of Golay correlator / MF.

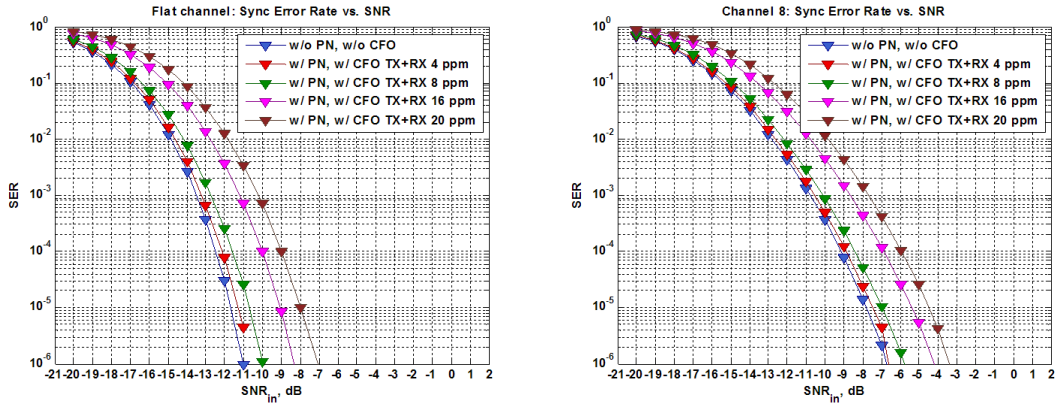

(a) Frequency flat channel **(b) IEEE 802.11ad channel #8**

Figure 2.2.3-22: Synchronization error rate vs. SNR performance in frequency flat and selective channels without and in presence of RF chain imperfections.

PHY type identification is done using both STF and CEF parts of the preamble. The decision between control PHY and SC/OFDM is done using STF. The STF signal is fed into both Ga and Gb branches of the Golay correlator / MF. Then the detector makes decision about PHY type depending on the branch where detection event is observed. If detector decides that SC/OFDM PHY preamble is received then it should make further distinguishing between SC and OFDM.

The decision between SC and OFDM PHY is done applying similar criterion as for synchronization. The PHY type identification exploits signal sign inversion from the last $-Ga_{128}$ sequence in STF and the first Ga_{128} sequence in CEF field for OFDM PHY and no sign inversion from the last $-Ga_{128}$ sequence in STF and the first $-Ga_{128}$ sequence in CEF for SC PHY (see Fig. 2.2.1.3-2, Fig. 2.2.1.4-1, and Fig. 2.2.1.5-1).

Figure 2.2.3-3 (a) shows receiver PHY type identification error rate versus SNR performance for SC and OFDM PHY. It is potted without RF chain imperfections and in presence of Phase Noise (PN) (applied at both transmitter and receiver sides) and Carrier Frequency Offset (CFO) equal to 4, 8, 16, and 20 ppm. Figure 2.2.3-3 (b) shows corresponding curves in case of IEEE 802.11ad channel #8. The SNR is introduced at the input of Golay correlator / MF.

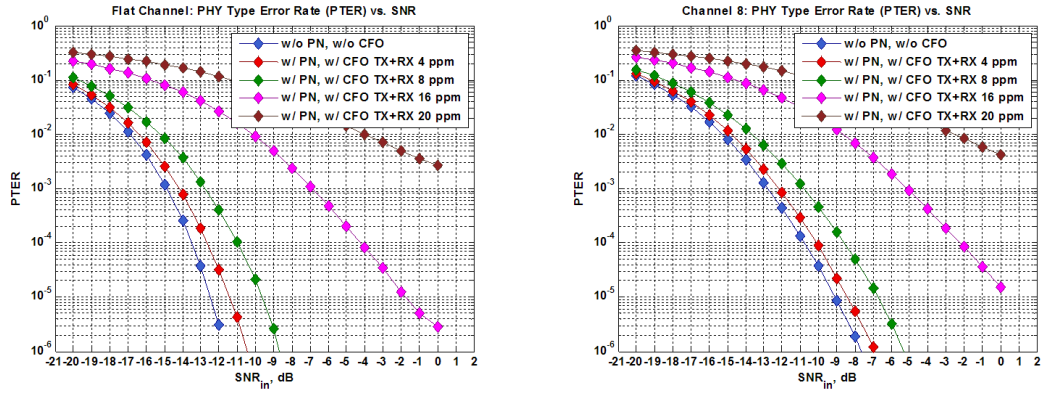

(a) Frequency flat channel **(b) IEEE 802.11ad channel #8**

Figure 2.2.3-3: PHY type identification error rate vs. SNR performance for SC and OFDM PHY in frequency flat and selective channels without and in presence of RF chain imperfections.

Initial Carrier Frequency Offset (CFO) estimation is done using STF field. The CFO estimation can be done applying autocorrelation (AC) algorithm exploiting repetitions of Ga_{128}/Gb_{128} sequences in the STF. In that case the knowledge about signal repetitions is used only. Another possibility is to use the knowledge about signal shape, apply matched filtering and make estimation at the output of MF. Both options are supported in the LLS platform. In order to estimate CFO for the signal at the output of MF, Luise-Reggiannini (L&R) estimation algorithm is used.

Note that CFO estimation can be done for different time lags equal to 1 or greater number of Sections Ga/Gb. Coarse CFO estimation may be done using small delay equal to D = 1 or 2 Ga/Gb Sections to avoid phase ambiguity. After coarse CFO estimation and compensation, fine CFO estimation may be done applying larger delays D.

Figure 2.2.3-4 (a) shows standard deviation of CFO estimation in ppm versus SNR (introduced per sample before MF) performance for L&R and autocorrelation (AC) algorithms without PN. Their performance is compared to the Cramer Rao Lower Bound (CRLB). L&R algorithm uses only coarse estimation with D = 2 and AC algorithm uses coarse estimation with D = 2 and fine estimation with D = 4. Figure 2.2.3-4 (b) shows L&R and AC algorithms performance in presence of PN.

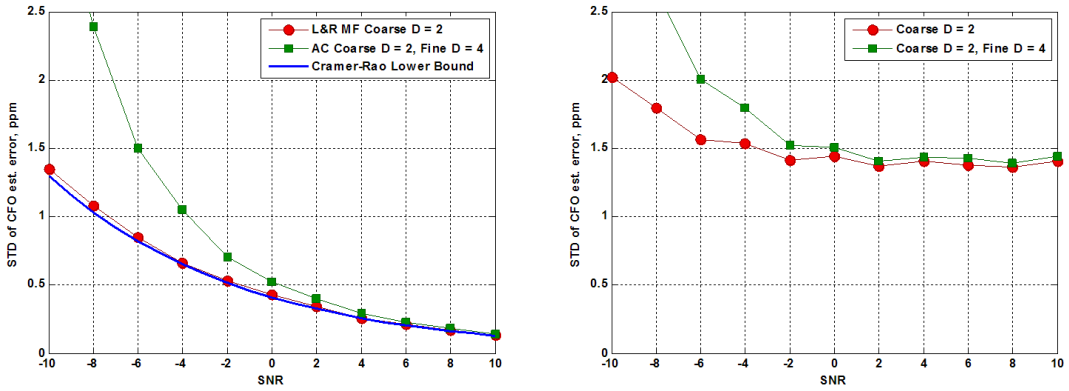

(a) Simulation results w/o PN **(b) Simulation results with PN**

Figure 2.2.3-4: CFO estimation algorithms performance with and without Phase Noise (PN).

Channel estimation is done using Gu_{512} and Gv_{512} sequences of the CEF field shown in Fig. 2.2.1.3-2 and Fig. 2.2.1.5-1. Channel estimation can be done in time domain using complementary property of Ga_{128} and Gb_{128} Golay sequences and applying Golay correlator. Another possibility is to do channel estimation in frequency domain and apply MF to Gu_{512} and Gv_{512} sequences. Both options are supported in the LLS platform.

Figure 2.2.3-5 (a) shows PSDU Packet Error rate (PER) vs. SNR (introduced per sample in time domain) performance comparison in case of ideal channel knowledge and channel estimation using frequency domain approach for frequency flat channel. PSDU length is equal to 8192 bytes. Figure 2.2.3-5 (b) shows similar comparison for the IEEE 802.11ad channel model #9.

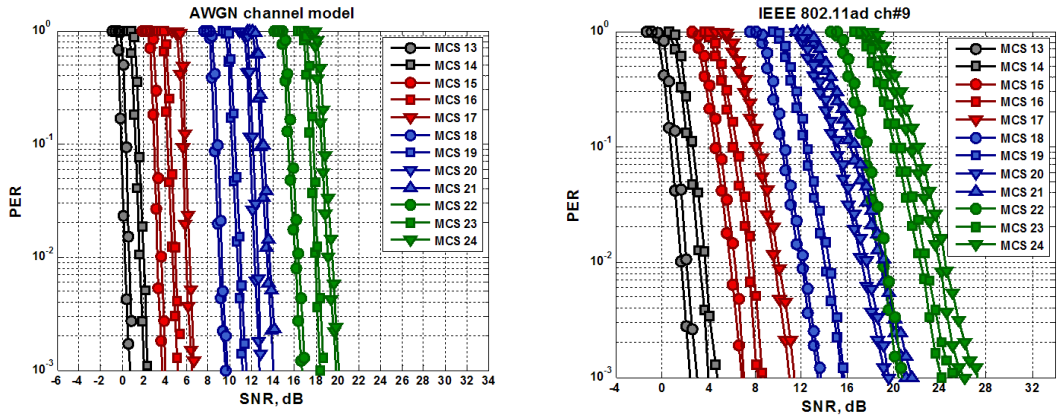

(a) Frequency flat channel **(b) IEEE 802.11ad channel #9**

Figure 2.2.3-5: PSDU Packet Error rate (PER) vs. SNR performance comparison in case of ideal channel knowledge and channel estimation using frequency domain approach.

For frequency flat channel degradation due to channel estimation is equal to ~ 0.3 dB and for IEEE 802.11ad channel #9 it is equal to ~0.3 – 0.45 dB.

2.2.4 Data Transmission Test Description

The purpose of data transmission test is to estimate IEEE 802.11ad frame demodulation and decoding performance for different channel models using header and payload data part of the frame.

Data processing block of the LLS platform performs the following functions:

1. Control PHY de-spreading and demodulation;
2. OFDM symbols demodulation applying FFT and converting back to the frequency domain;
3. OFDM symbols Zero Forcing (ZF) equalization in frequency domain;
4. SC symbols equalization in frequency domain applying the following steps:
    a. FFT to convert symbol to frequency domain;
    b. Linear Minimum Mean Square Error (LMMSE) equalization and bias compensation;
    c. IFFT to convert symbol back to time domain;
5. Residual CFO tracking using GIs in time domain for SC modulation and pilots in frequency domain for OFDM modulation method, CFO tracking is not needed for control PHY since it uses DBPSK modulation;
6. Digital to Analog Converter (DAC) and Analog to Digital Converter (ADC) Sampling Frequency Offset (SFO) estimation and tracking in time domain (actually CFO error is estimated and SFO error is calculated using CFO assuming that they are derived from the same reference oscillator as specified in the standard);
7. Phase Noise (PN) estimation and compensation;
8. Power Amplifier (PA) non-linearity estimation and compensation (nonlinear equalization);
9. QAM symbols demapping;
10. Header and data payload bit stream LDPC decoding and descrambling;

Figure 2.2.4-1 shows Packet Error Rate (PER) vs. SNR performance comparison for SC and OFDM modulations in case of frequency flat and IEEE 802.11ad channel #8 and 9 models. These curves were simulated for ideal channel knowledge and without RF imperfections. SNR for SC modulation is introduced per sample (chip) in time domain and SNR for OFDM modulation is introduced per subcarrier in frequency domain.

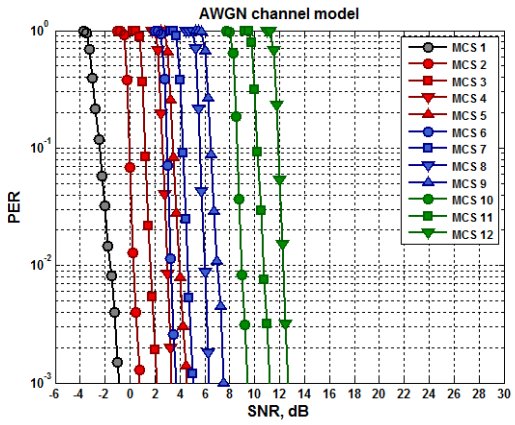

(a) SC – frequency flat channel

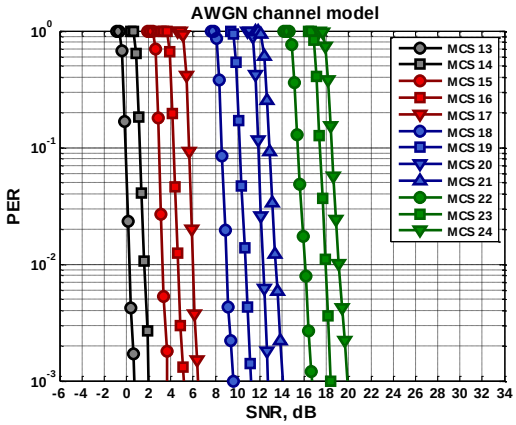

(b) OFDM – frequency flat channel

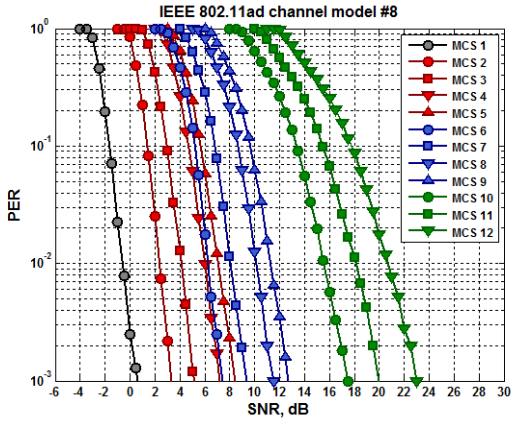

(c) SC – IEEE 802.11ad channel #8

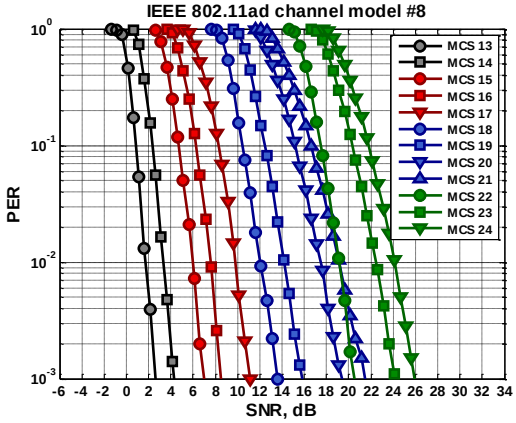

(d) OFDM – IEEE 802.11ad channel #8

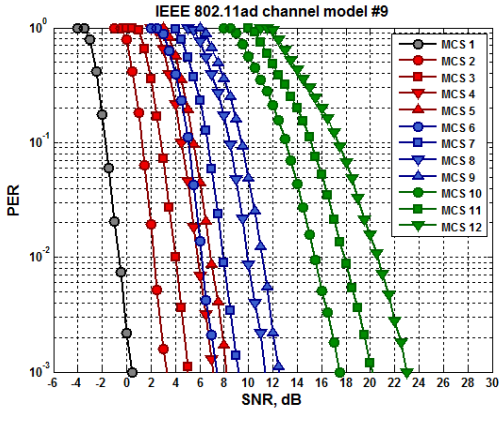

(e) SC – IEEE 802.11ad channel #9

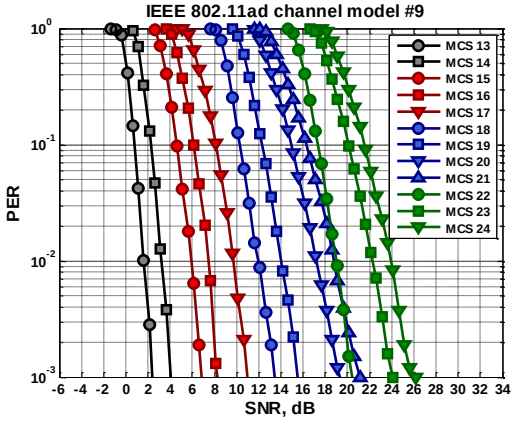

(f) OFDM – IEEE 802.11ad channel #9

Figure 2.2.4-1: PSDU Packet Error Rate (PER) vs. SNR performance for SC and OFDM modulations in case of frequency flat, IEEE 802.11ad channel #8 and 9.

Figure 2.2.4-2 shows an example of transmit spectral mask test for SC and OFDM modulations for the Power Amplifier (PA) Output Back-off (OBO) equal to -1.0 dB and -1.5 dB accordingly. The estimations of the spectrum were done for Resolution Bandwidth (RBW) equal to 1 MHz and Video Bandwidth (VBW) equal to 100 kHz as defined in the standard, [7]. The estimated spectrums are compared to the mask specified in the standard.

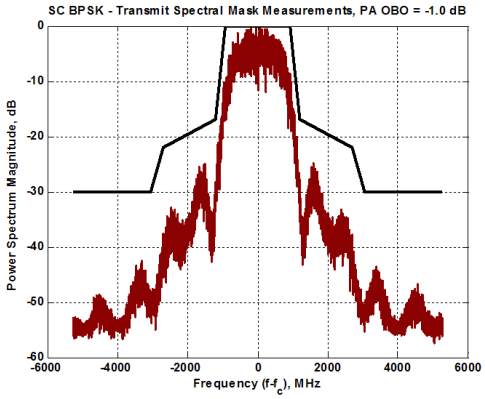

(a) BPSK SC – OBO = -1.0 dB

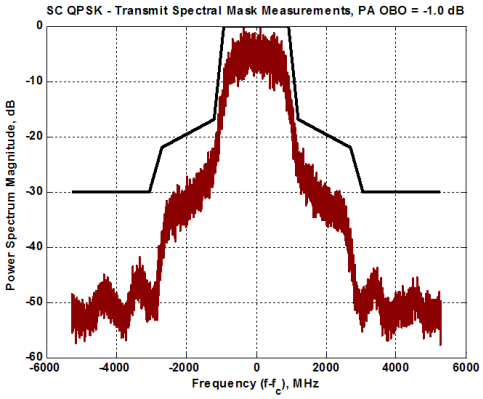

(b) QPSK SC – OBO = -1.0 dB

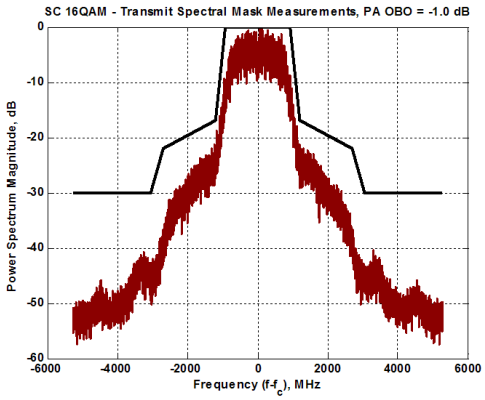

(c) 16QAM SC – OBO = -1.0 dB

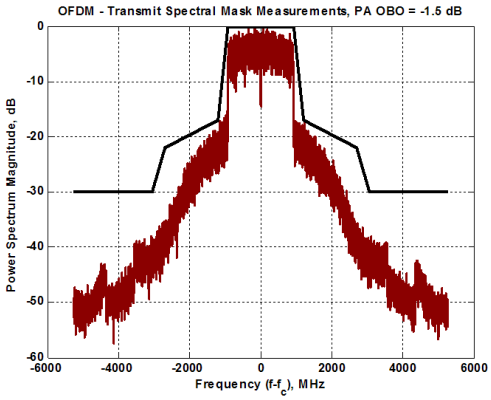

(d) OFDM - OBO = -1.5 dB

Figure 2.2.4-2: Example of transmit spectral mask test for SC and OFDM modulations.

2.3 Interface between LLS and SLS

2.3.1 Physical layer abstraction method

Link performance prediction is based on determining the function which maps multiple physical SINR observations to single "wide-band" metric which then can be converted to BLER by means of the second mapping function (usually an AWGN reference).

The physical layer abstraction method used in SLS is based on the Mean Mutual Information per coded Bit (MMIB) metric [11] and includes two steps (see Fig. 2.3.1-1)

1. Calculation of MMIB metric for the given post-processing SINR values corresponded to each of *N* subcarriers transmitting the transport block.
2. MMIB to BLER mapping

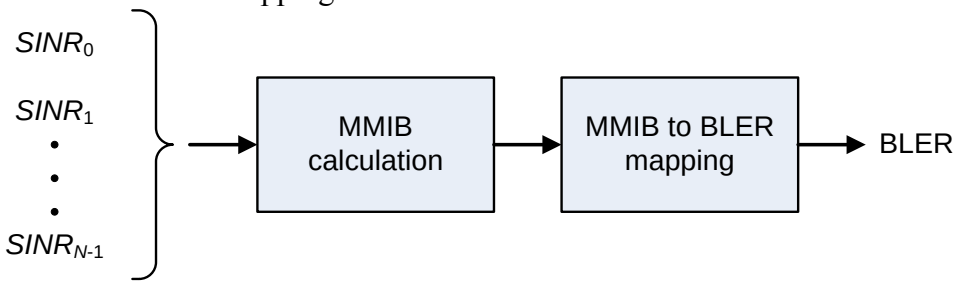

Figure 2.3.1-1: Illustration of physical layer abstraction method.

2.3.1.1 MMIB calculation

The first mapping function can be defined as

$$MMIB = \frac{1}{N}\sum_{n=1}^{N} I_m\left(SINR_n\right),$$

where $I_m\left(SINR_n\right)$ is the mutual information per bit function for subcarrier *n*, *m* is the modulation order, *N* is the number of subcarriers.

Assuming ideal interleaving, the system can be seen equivalently as *m* parallel independent and memoryless binary-input bit-channels [12]. Considering the computation of log-likelihood ratio of the i^{th} bit comprising the symbol using the following expression

$$LLR\left(b_i\right) = \ln\left(\frac{P\left(b_i = 1|y\right)}{P\left(b_i = 0|y\right)}\right),$$

where *y* is the received signal, the mutual information per bit of the equivalent bit-channel for SISO systems can be expressed as

$$I(b, LLR) = \frac{1}{m}\sum_{i=1}^{m} I\left(b_i, LLR\left(b_i\right)\right),$$

where $I\left(b_i, LLR\left(b_i\right)\right)$ is the mutual information between input bit to the QAM mapper and output LLR for i^{th} bit in the modulation map.

For BPSK modulation in the AWGN channel the received signal can be represented as

$$y = x + n,$$

where n is Gaussian distributed with mean zero and variance $\sigma_n^2 = 1/(2E_s/N_0)$ (double-sided noise power spectral density) and $x \in \{\pm 1\}$. So the expression for LLR can be simplified to

$$LLR = \frac{2}{\sigma_n^2}(x+n),$$

and can also be formulated as

$$LLR = \mu x + n_1$$

with

$$\mu = \frac{2}{\sigma_n^2}$$

and n_1 being Gaussian distributed with mean zero and variance

$$\sigma = \frac{4}{\sigma_n^2}$$

Since the LLR satisfies $\mu = \sigma^2/2$, the expression for $I(b, LLR)$ simplifies to

$$I(b,LLR) = \frac{1}{2}\sum_{b=0,1}\int_{-\infty}^{+\infty} p_{LLR}(z|b)\log_2\left(\frac{2\,p_{LLR}(z|b)}{p_{LLR}(z|b=0)+p_{LLR}(z|b=1)}\right)dz =$$

$$= 1 - \int_{-\infty}^{+\infty}\frac{1}{\sqrt{2\pi\sigma}}e^{-(z-\sigma^2/2)^2/2\sigma^2}\cdot\log_2\left(1+e^{-z}\right)dz = J(\sigma) = J(\sqrt{8E_s/N_0}) = J(\sqrt{8SINR}),$$

where

$$J(\sigma) = 1 - \int_{-\infty}^{\infty}\frac{1}{\sqrt{2\pi\sigma}}e^{-(v-\sigma^2/2)^2/2\sigma^2}\cdot\log_2\left(1+e^{-v}\right)dv.$$

There is an easy way to compute the function $J(x)$ by using the following approximation [13]

$$J(x) \approx \begin{cases} a_1x^3 + b_1x^2 + c_1x, & if\ x \le 1.6363 \\ 1 - exp(a_2x^3 + b_2x^2 + c_2x + d_2) & if\ 1.6363 \le x \le \infty \end{cases},$$

where $a_1 = -0.0421061, b_1 = 0.209252$ and $c_1 = -0.00640081$ for the first approximation, and where $a_2 = 0.00181491, b_2 = -0.142675, c_2 = -0.0822054$ and $d_2 = 0.0549608$ for the second approximation.

For higher-order modulations the LLR PDF can be approximated with the mixture of Gaussian distributions defined by individual means and standard deviations. If the LLR distribution can be approximated by the Gaussian distributions, the MIB can be

asymptotically expressed by the sum of $J(x)$ functions. The approximations can be obtained by numerical optimization [11].

The corresponding expressions for $I_m(SINR_n)$ computation for different modulations are summarized below.

Table 2.3.1.1-1: MI functions for different modulations

Modulation	**MI Function**
BPSK	$I_1(\gamma)=J\left(\sqrt{8\gamma}\right)$
QPSK	$I_2(\gamma)=J\left(2\sqrt{\gamma}\right)$
16 QAM	$I_4(\gamma)=\frac{1}{2}J\left(0.8\sqrt{\gamma}\right)+\frac{1}{4}J\left(2.17\sqrt{\gamma}\right)+\frac{1}{4}J\left(0.965\sqrt{\gamma}\right)$
64 QAM	$I_6(\gamma)=\frac{1}{3}J\left(1.47\sqrt{\gamma}\right)+\frac{1}{3}J\left(0.529\sqrt{\gamma}\right)+\frac{1}{3}J\left(0.366\sqrt{\gamma}\right)$

2.3.1.2 MMIB to BLER mapping

The devices can store the AWGN reference fitting curves for MMIB to BLER mapping for each MCS. But the alternative way is to approximate these curves with a parameterized function. For physical layer abstraction used in SLS, the approximation by Gaussian cumulative function was used

$$BLER=\frac{1}{2}\left[1-erf\left(\frac{MMIB-X_1}{\sqrt{2}X_2}\right)\right], X_2\neq 0.$$

So the MMIB to BLER mapping requires only two parameters for each MCS. Such an approximation provides a close fit to the AWGN performance curve.

2.3.2 Mm-wave PHY abstraction

For the link to system mapping used in SLS the PER vs. SNR curves for AWGN channel obtained by means of LLS (Figures 2.2.4-1 a, b) were used. According to the method described in Section 2.3.1 these curves were converted into the PER vs. MMIB performance and then approximated by Gaussian cumulative functions. The computed parameters X_1 and X_2 for each MCS are presented in the tables below.

The parameters in Tables 2.3.2-1 and 2.3.2-2 were obtained under the assumption of fixed packet size 8192 bytes what complies the 802.11ad standard

Table 2.3.2-1: PHY abstraction parameters for SC modulations under the assumption of fixed packet size

MCS index	Modulation order	Code rate	Spectral efficiency	X_1	X_2	Payload, bytes
1	1	0.5000	0.5000	0.4739	0.0483	8192
2	1	0.5000	0.5000	0.6944	0.0202	8192

3	1	0.6250	0.6250	0.7878	0.0198	8192
4	1	0.7500	0.7500	0.8781	0.0127	8192
5	1	0.8125	0.8125	0.9151	0.0141	8192
6	2	0.5000	1.0000	0.6946	0.0195	8192
7	2	0.6250	1.2500	0.7878	0.0200	8192
8	2	0.7500	1.5000	0.8784	0.0125	8192
9	2	0.8125	1.6250	0.9134	0.0158	8192
10	4	0.5000	2.0000	0.6635	0.0150	8192
11	4	0.6250	2.5000	0.7570	0.0189	8192
12	4	0.7500	3.0000	0.8499	0.0154	8192

Table 2.3.2-2: PHY abstraction parameters for OFDM modulations under the assumption of fixed packet size

MCS index	Modulation order	Code rate	Spectral efficiency	X_1	X_2	Payload, bytes
13	1	0.5000	0.5000	0.6969	0.0170	8192
14	1	0.6250	0.6250	0.7864	0.0213	8192
15	2	0.5000	1.0000	0.6970	0.0171	8192
16	2	0.6250	1.2500	0.7867	0.0215	8192
17	2	0.7500	1.5000	0.8770	0.0140	8192
18	4	0.5000	2.0000	0.6621	0.0171	8192
19	4	0.6250	2.5000	0.7558	0.0199	8192
20	4	0.7500	3.0000	0.8516	0.0137	8192
21	4	0.8125	3.2500	0.8903	0.0169	8192
22	6	0.6250	3.7500	0.7519	0.0204	8192
23	6	0.7500	4.5000	0.8495	0.0153	8192
24	6	0.8125	4.8750	0.8887	0.0168	8192

The parameters in Tables 2.3.2-3 and 2.3.2-4 were obtained under the assumption of fixed time allocation 1ms what is equal to 1 LTE subframe.

Table 2.3.2-3: PHY abstraction parameters for SC modulations under the assumption of fixed time allocation

MCS index	Modulation order	Code rate	Spectral efficiency	X_1	X_2	Payload, bytes

1	1	0.5000	0.5000	0.4612	0.0468	48125
2	1	0.5000	0.5000	0.6964	0.0199	96250
3	1	0.6250	0.6250	0.7928	0.0189	120310
4	1	0.7500	0.7500	0.8814	0.0140	144380
5	1	0.8125	0.8125	0.9206	0.0138	156410
6	2	0.5000	1.0000	0.7053	0.0176	192500
7	2	0.6250	1.2500	0.7998	0.0202	240630
8	2	0.7500	1.5000	0.8880	0.0126	288750
9	2	0.8125	1.6250	0.9253	0.0151	312810
10	4	0.5000	2.0000	0.6732	0.0207	385000
11	4	0.6250	2.5000	0.7743	0.0217	481250
12	4	0.7500	3.0000	0.8675	0.0137	577500

Table 2.3.2-4: PHY abstraction parameters for OFDM modulations under the assumption of fixed time allocation

MCS index	Modulation order	Code rate	Spectral efficiency	X_1	X_2	Payload, bytes
13	1	0.5000	0.5000	0.6976	0.0169	86625
14	1	0.6250	0.6250	0.7901	0.0207	108280
15	2	0.5000	1.0000	0.7017	0.0203	173250
16	2	0.6250	1.2500	0.7995	0.0195	216560
17	2	0.7500	1.5000	0.8861	0.0137	259880
18	4	0.5000	2.0000	0.6757	0.0176	346500
19	4	0.6250	2.5000	0.7740	0.0198	433130
20	4	0.7500	3.0000	0.8647	0.0153	519750
21	4	0.8125	3.2500	0.9084	0.0167	563060
22	6	0.6250	3.7500	0.7755	0.0215	649690
23	6	0.7500	4.5000	0.8693	0.0137	779630
24	6	0.8125	4.8750	0.9103	0.0157	844590

The approximation accuracy of PHY abstraction for SC and OFDM modulations is shown on Figure 2.3.2-1.

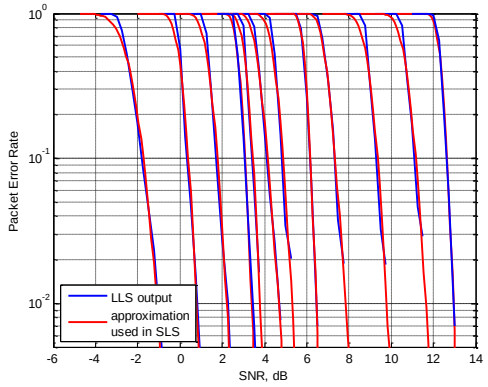

(a) SC – frequency flat channel

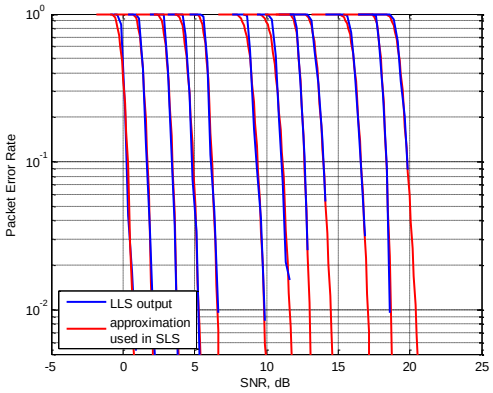

(b) OFDM – frequency flat channel

Figure 2.3.2-1: Packet Error rate (PER) vs. SNR performance comparison for AWGN channel.

3 System level simulator

3.1 Parameters for system level simulator

In this section, fundamental parameters for the system level simulation are described. The system which focusing on is an mm-wave overlay HetNet and it is constructed by wide area macro base station (macro BS) and small area coverage base stations (smallcell BS). It is assumed that macro BS LTE system works in 2G Hz band and smallcell BS LTE system works in 3.5GHz band and the 802.111 ad system works in 60 GHz band. Parameters are based on the 3GPP standards and IEEE 802.11ad standards. Moreover, outputs of other project tasks are also integrated in particular the new mm-wave channel model. The purpose of the system level simulation is to investigate the potential of the mm-wave overlay HetNet. Therefore some parameters e.g. CSI feedback error, signal overhead, etc. are not part of this deliverable.

3.1.1 LTE standard macro and smallcell parameters

Parameters for LTE standard macro and smallcell are summarized in Table 3.1.1-1.

TABLE 3.1.1-1 LTE Macro and Smallcell Parameters

Parameter	Macro cell	Small cell
Cell Layout	Hexagonal (ISD: 500 m)	random drop
Carrier Frequency [GHz]	2.0	3.5
Available bandwidth [MHz]	10	100
Number of resource blocks	50	500
BS Tx Power [dBm]	43	30
BS Antenna Height [m]	25	10
Anttena Pattern	3 Sector	Omni
Antenna gain [dBi]	17	5
Number of antennas	4	4
Delay spread [μs]	0.363	0.129
Path Loss [dB] (d in [m])	128.1+37.6*log10(d)	140.7+36.7*log10(d)
Transmission scheme	SVD-MIMO	
Shadowing	log normal distribution with decorrelation distance: 50m for macro, 13m for smallcell standard deviation: 6dB for macro, 4dB for smallcell	
UE mobility	3 km/h linear walk	

LTE parameters are based on the 3GPP standards [14, 15]. We assume FD-LTE and perfect CSI feedback and the effects of H-ARQ are not considered. Additionally, any signalling overheads are not included.

3.1.2 Mm-wave small cell

Parameters for mm-wave small cell are summarized in Table 3.1.2-1.

TABLE 3.1.2-1 Mm-wave Smallcell Parameters

Parameter	Value
Cell Layout	Hexagonal or random drop
Carrier Frequency [GHz]	60
Available bandwidth [MHz]	2160
Number of subcerriers	512 (for user data transmission: 336)
BS Tx Power [dBm]	10 (Japan regulation), 22 (EU regulation)
BS Antenna Height [m]	4
Anttena Pattern	IEEE 802.11ad complient [9]
Number of antennas	8x32 (8x2x16) or 8x64 (8x2x32) full adaptive array antenna. Notice: The antenna array is constructed by 8x2 antenna array modules. Each antenna array module creates one pencil beam and transmits one signal stream. Only one beam is allocated to one user.
Delay spread [μs]	0.015
Path Loss [dB] (d in [m])	$\begin{cases} 82.02 + 23.6\log_{10}(d/d_0), d \geq d_0 \\ 82.02 + 20\log_{10}(d/d_0), d < d_0 \end{cases}$ d_0 :reference distance: 5m [17]
Transmission scheme	SVD-MIMO (Multi user MIMO is option)
Shadowing	log normal distribution with standard deviation: 5dB
UE mobility	3 km/h linear walk

Mm-wave parameters are based on the IEEE 802.11ad standard [9]. In this simulator, only OFDM transmission is available. In multi-user MIMO transmission case, one antenna array module creates one directional beam towards each users.

3.2 Resource management framework

3.2.1 Network architecture and C/U splitting

One of the key elements of the network architecture in the MiWEBA project is the data and control plane separation that is called C/U splitting. As explained in Deliverable 3.1 [16], the architecture for C/U splitting in 3rd Generation Partnership Project (3GPP) is considered as the basis to realize C/U splitting scheme for the mm-wave Overlay HetNets. Though for MiWEBA architecture, additional enhancements are required as studied in Deliverable 3.1 [16].

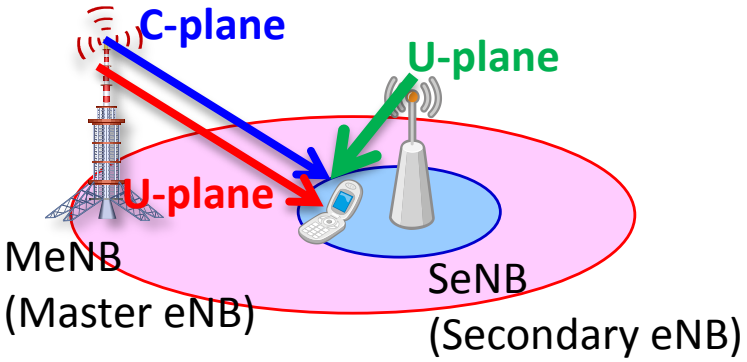

Figure 3.2.1-1 Overview of C/U-plane splitting [16]

In the C/U plane splitting scheme the UEs can get C-plane data via MeNB (Master eNB) and U-plane data via MeNB and SeNB (Secondary eNB) as shown in Figure 3.2.1-1. Typically, MeNB and SeNB are the macro eNB and smallcell eNB, respectively. Owing to the scheme, both stable and high throughput communication will be realized. To be more specific, the UE can keep a main control-plane connection active, typically within a long-range macro cell, and activate user-plane connections to different base stations which provide the best data traffic bearers according to both user and network status.

The general concept of C/U-plane splitting scheme is independent of carrier frequencies. Nonetheless, it is necessary to enhance the architecture for the MiWEBA HetNets by introducing more flexibility and multiple design choices. Particularly, extended network functionalities are required to deal with millimeter wave C/U-plane split. The enhancement of conventional LTE C/U-plane splitting scheme is being studied in Task 3.1 and the outputs will be presented in Deliverable 3.2 “Extension of control plane.”

3.2.2 Mobility management (cell association for U-plane)

In the C/U plane splitting scheme, basically the network selects the access points for UEs. This architecture can provide a more flexible and intelligent cell association and mobility management taking into account the status of the whole network.

User-plane connections can be established with both macro cells and small cells leaving room for the development of optimized resource allocation algorithms. In general, two types of mobility can be identified, a so-called small-scale mobility, where the UE moves within the coverage of a single control-plane macro cell and performs user-plane handovers through small cells, while traditional mobility occurs when the UE crosses macro cell boundaries [16]. Mobility management among different data networks during active communication sessions is a challenging issue. However, the advantage of the new system architecture is that the network has the full control of resource selection.

On the other hands, the directionality of the millimeter-wave links requires a new kind of mobility support on the link or beam level. This is discussed as beam forming tracking. The beam forming tracking is a crucial part of the millimeter-wave connectivity. The directional millimeter-wave link continuously changes, and therefore, the beam forming vectors must be updated frequently. Such information is

needed on both ends of the millimeter-wave link. This functionality is therefore located at the smallcell control plane [16].

3.2.3 Radio resource control

When the UE is in idle state it is connected to the legacy macro base station. It is assumed that the UE is not connected to a millimeter-wave link when idle, in order to reduce the energy consumption. This reduce both UE power consumption and network power consumption. In fact, the millimeter-wave base stations can be considered to be switched off when no data session is active. When the session is initiated by a request from the macro base station, the macro C-plane alerts the UE. Then the UE and the appropriate small cell initiate the directional millimeter-wave connection. This process has been summarized in Figure 3.2.3-1.

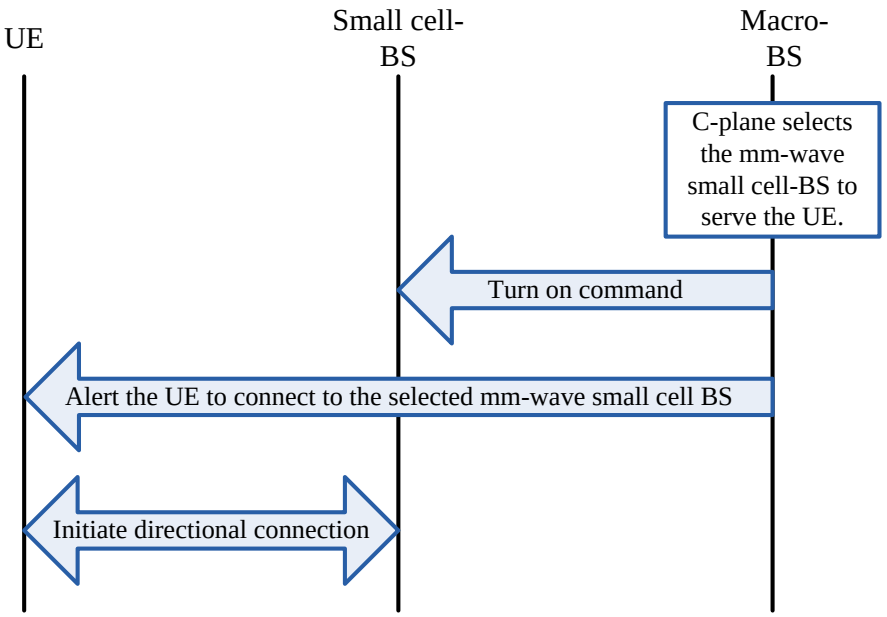

Figure 3.2.3-1 Initiation of the directional millimeter-wave connection

For the resource allocation, the small cell polls the UEs for their demand to communicate and allocates time slots. The macro cell C-plane orchestrates the operation of millimeter-wave small cells and manages the wireless medium access of millimeter-wave devices. It also can be used to realize scenarios where a millimeter-wave base station simultaneously communicates with multiple UEs. In addition, interference coordination techniques including coordinated beam forming are considered to further improve the wireless resource exploitation.

3.3 System level simulator

System level simulator was developed to evaluate two scenarios: full-buffer scenario and non-full-buffer scenarios. Full-buffer scenario evaluates the upper-bound performance of the system where mm-wave links are assumed to be exploited over the entire evaluation period. However such situation occurs only when there are many high traffic users. To evaluate the performance of mm-wave overlay HetNet in realistic case, it is also important to introduce non-full-buffer scenario. Details on their procedure and execution parameters are described below.

3.3.1 SLS procedure

The procedure of LTE and millimeter-wave HetNets SLS is presented in the Figure 3.3.1-1. This procedure is common for both full-buffer and non-full-buffer scenarios. The configuration parameters are used for SLS initialization. The simulator initialization part consists of such functional blocks as *Simulation configuration*, *Deployment creation*, *User association* and *Warm-up frames processing*. As the simulation setup ends the SLS core begins where the main simulations are carried out. SLS core is a loop where each iteration is one LTE sub-frame. Each subframe consists of *User scheduling*, *Channel generation*, *Rx processing* and *Feedback generation*. Simulation results are collected on each iteration and after the end of the loop are saved.

Detail description of each functional block is provided in the following sections.

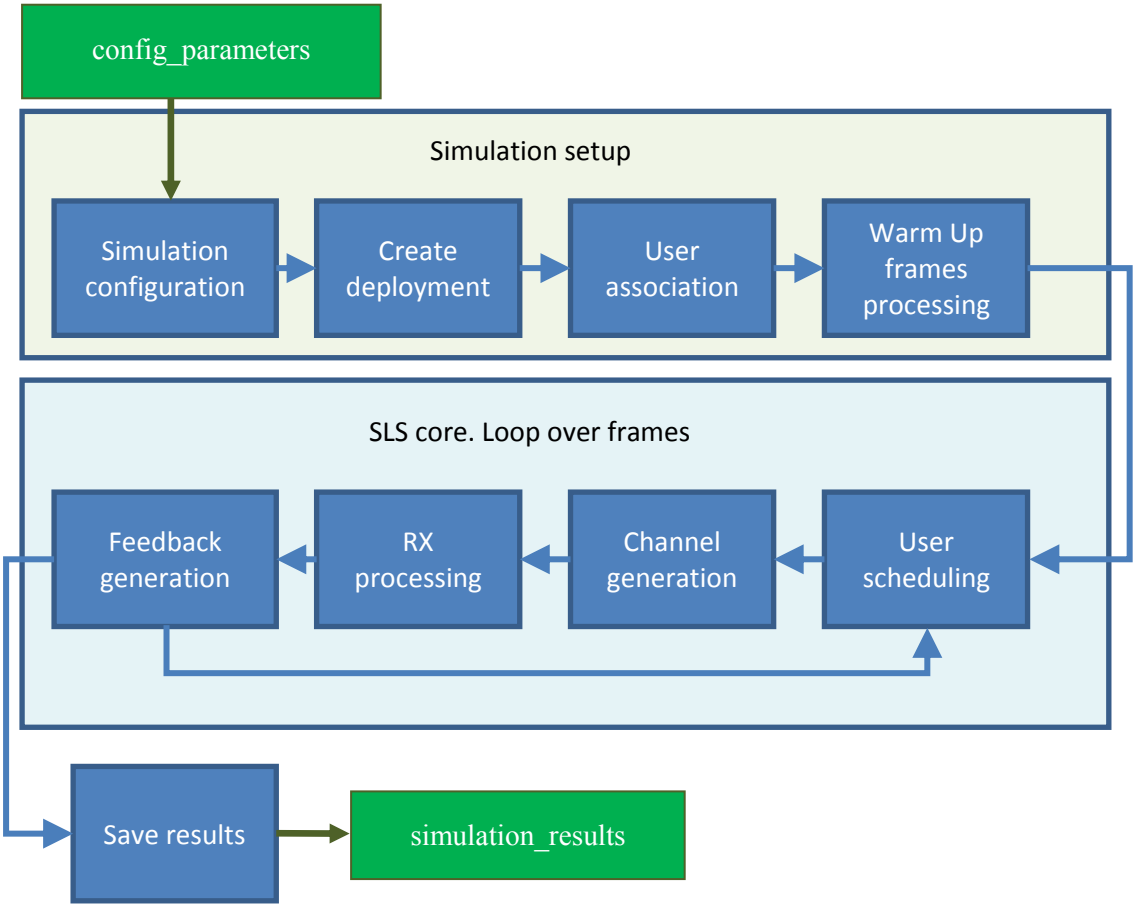

Figure 3.3.1-1 SLS procedure

3.3.2 Simulations setup

3.3.2.1 Simulation configuration

Functions of this block read the configuration which is the input of SLS and define the common simulation parameters and the specific parameters for the technologies (LTE and mm-wave) which are enabled for current simulation. The LTE parameters are configured according to 3GPP specifications [14, 2, 3, 4]. The numerology for mm-wave system parameters is presented in Table 3.3.2.1-1.

As the extensive measurement results on channel delay characteristics [17] have shown, the mmWave system, which is targeted at outdoor communications requires some modifications of IEEE 802.11ad parameters to make mm-wave frames transmission synchronous with LTE frames. In the Table 3.3.2.1-1 the comparison of WiGig and LTE parameters is presented. In the last column the proposed parameters of new mmWave outdoor system are presented.

Table 3.3.2.1-1 Mm-wave system parameters

Parameter	**Wi-Gig**	**LTE Rel-11**			**mm-wave LTE with very high throughput**
System bandwidth	2160 MHz	5 MHz	10 MHz	20 MHz	2000 MHz
Channels	3	1	1		1
FFT size	512	512	1024	2048	1024
Subcarrier frequency spacing	5.15625 MHz	0.015 MHz			3.0 MHz
OFDM sample rate	2640 MHz	7.68 MHz	15.36 MHz	30.72 MHz	3072 MHz
Total Number of subcarriers (OFDM)	352	300	600	1200	600
Number of data subcarriers (OFDM)	336	270 in average	540 in average	1080 in average	540
IDFT/DFT period (OFDM / SC)	0.194 µs / 0.292 µs	66.67 µs			330 ns
Guard Interval duration (OFDM / SC)	48.4 ns / 36.5 ns	4.69 / 5.21 µs			70 ns
Symbol Interval (OFDM / SC)	0.242 µs / 0.328 µs	71.36 / 71.88 µs			400 ns
Frame duration	Variable (70-700 µs for 8192 bytes)	10 ms			10 ms

- Non-full-buffer scenario:

Additionally in non-full-buffer scenario, traffic demand of each users are set. Mm-wave system can transmit a huge amount of data in a blink. However since the coverage is limited, only a few users can get benefits. In order to use mm-wave resource effectively, users whose traffic demand is relatively high should be accommodated into mm-wave system appropriately. This simulator employs Gamma distribution traffic model [18] which is made from actual traffic data in urban area, Japan. Figure 3.3.2.1-1 is a CDF of the user traffic. If the property of traffic

distribution will not change in the future, we can predict future traffic demand by controlling the scale parameter of Gamma distribution.

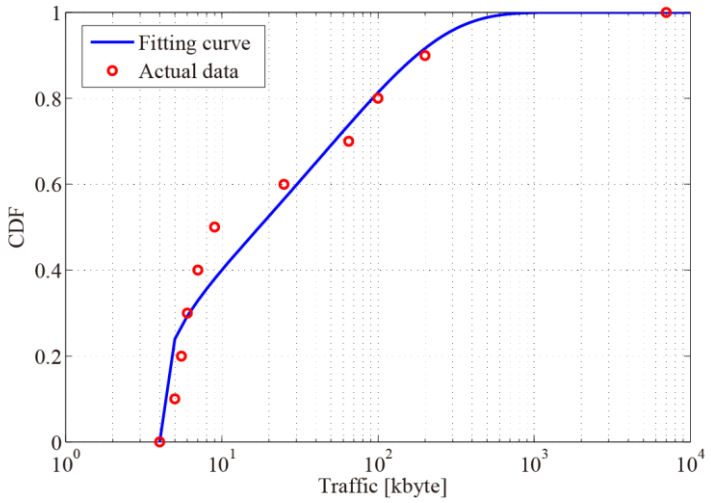

Figure 3.3.2.1-1 Traffic distribution CDF

3.3.2.2 Deployment creation

Functions of this block deploy base stations (Macro and Small cells) and UEs according to defined simulation scenario. Supported deployment scenarios are different as for full-buffer and non-full-buffer scenarios as follows.

- Full-buffer scenario:

The following scenarios are supported in full-buffer scenario: homogeneous LTE or mm-wave hexagonal deployment, heterogeneous LTE-only and LTE and mm-wave deployments (Fig. 3.3.2.2-1). The UE dropping can be uniform or clustered (for HetNet scenarios), when a certain percentage of users are dropped near the small cells.

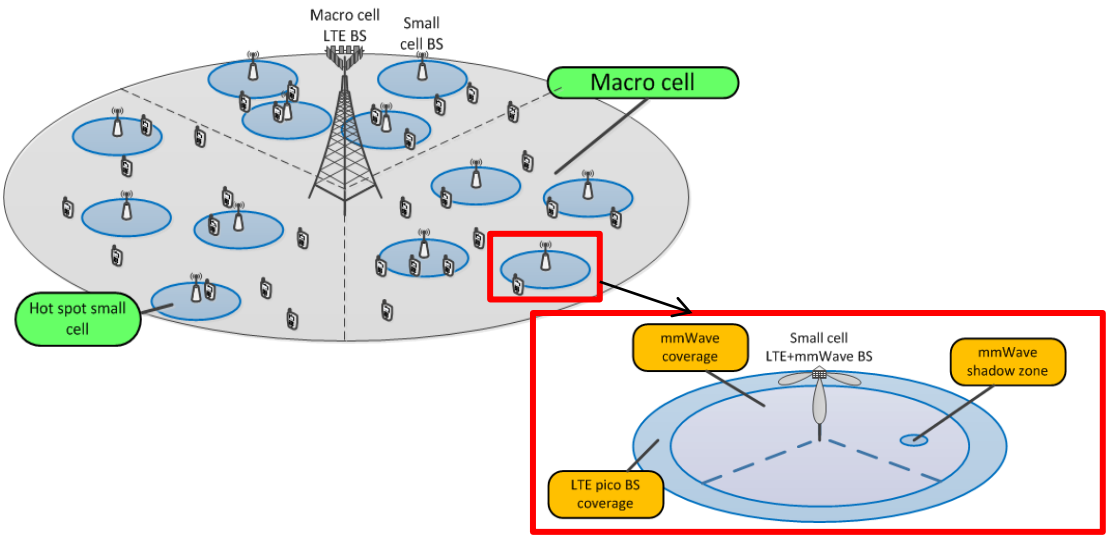

Figure 3.3.2.2-1 Deployment scenarios

- Non-full-buffer scenario:

In non-full-buffer scenario, 7 macro base stations are deployed in hexagonal grid. After that smallcell BSs are deployed randomly. Figure 3.3.2.2-2 shows the BS deployment condition. Blue dot indicates macro BS and green dots indicate smallcell BSs.

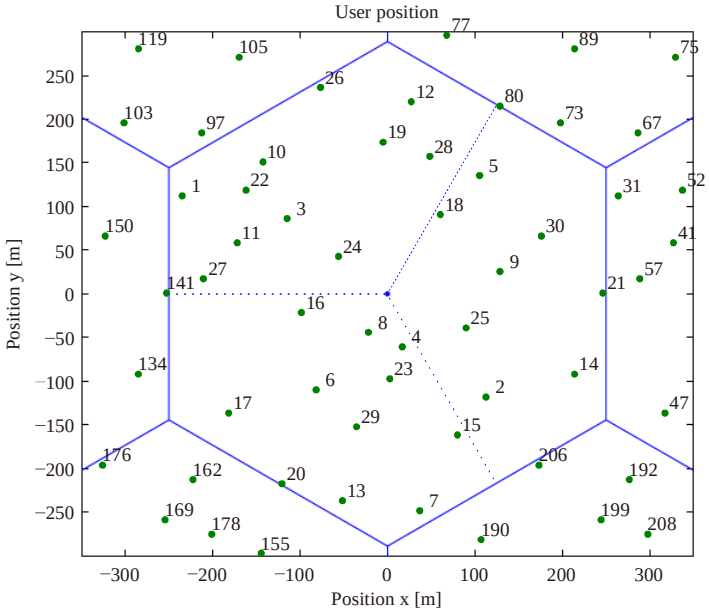

Figure 3.3.2.2-2 BS deployment condition

UEs are uniformly deployed in a target macro cell area and their moving directivity and orientation are also set at this step.

3.3.2.3 User association

- Full-buffer scenario:

For simple scenarios, such as LTE-only homogeneous and heterogeneous or mm-wave-only homogeneous scenario, cell selection is based on the received signal strength.

Since mm-wave always provides much higher performance in the case of heterogeneous LTE and mm-wave HetNet scenario, it is tried to associate all UEs satisfying minimum requirements to mm-wave BS. So if the UE is able to associate to mm-wave BS he will. At first the mm-wave BS with the highest SNR is chosen, then it is checked whether this SNR is higher than a predefined threshold. The threshold corresponds to minimal mm-wave MCS to be sure that the mm-wave transmission will not fail. If SNR is less than the threshold, this UE associates with LTE.

An abstraction of UE blockage is also introduced at this step. There is a probability that the UE can be in the mm-wave shadow zone. All UEs appeared to be in shadow zone also associate with LTE.

- Non-full-buffer scenario:

On the other hand in non-full-buffer scenario, UEs not always demand huge traffic therefore mm-wave is only effective for specific UEs. In order to exploit the potential of mm-wave, we employ combinatorial based cell association method. This association chooses the best user combination which can maximize system rate by solving the combinatorial optimization problem [14].

3.3.2.4 Warm Up frames processing

Warm up simulations represents several iterations of SLS core. They are needed to get first feedback and to put SLS into the steady state. The results for these simulations will not be taken into account.

3.3.3 SLS core and Loop over frames

Each of the blocks of this part of SLS is reused independently for each technology (LTE and mm-wave) which is enabled for current simulation.

3.3.3.1 User scheduling

- Full-buffer scenario:

In full-buffer scenario, multi-user (MU) greedy scheduling based on proportional fair (PF) metric is used. For MU group the best UEs are picked up one by one considering maximization of total group PF metric. Channel quality information and channel state information obtained from user feedback are used. During the scheduling the beam forming vectors are defined, using the interference mitigation techniques applied to TX side such as zero forcing if enabled.

- Non-full-buffer scenario:

In this block each BS performs user scheduling based on proportional fair (PF) metric [19]. Each BSs calculate PF metric and allocate resources to users who can achieve the highest PF metric.

$$\hat{i} = \arg\max_{i=1,2,\ldots N_{\mathrm{UE}}} \frac{R_i(t)}{T_i(t)}$$

$$T_i(t) = \left(1 - \frac{1}{t_c}\right) T_i(t-1) + \frac{1}{t_c} R_i(t) \times I\{\hat{i} = i\}$$

Where $R_i(t)$ and $T_i(t)$ are instantaneous user rate and average user rate of the i th UE respectively. N_{UE} is the total number of UEs in a cell. t_c is a time window of the averaging filter and $I\{\cdot\}$ is an indicator function.

3.3.3.2 Antenna gain calculation

According to the BS and UE positions, all distances and relative angles between BS and UE can be calculated. Path loss and antenna gain are calculated by using these geometric parameters. Antenna beam pattern of LTE macro BS is 3-sectorized pattern given as follows,

$$A_{\mathrm{H}}(\varphi) = -\min\left[12\left(\frac{\varphi}{\varphi_{3\mathrm{dB}}}\right), A_m\right], \varphi_{3\mathrm{dB}} = 70^\circ, A_m = 25\mathrm{dB}$$

$$A_{\mathrm{V}}(\theta) = -\min\left[12\left(\frac{\theta-\theta_{\mathrm{etilt}}}{\theta_{3\mathrm{dB}}}\right), SLA_v\right], \theta_{3\mathrm{dB}} = 10^\circ, \theta_{\mathrm{etilt}} = 15^\circ, SLA_v = 20\mathrm{dB}$$

$$A(\varphi,\theta) = -\min\{-[A_{\mathrm{H}}(\varphi) + A_{\mathrm{V}}(\theta)], A_m\}$$

where $\varphi_{3\mathrm{dB}}$ and $\theta_{3\mathrm{dB}}$ are horizontal and vertical half beam width respectively, θ_{etilt} is a down tilt angle. Mm-wave antenna beam pattern is IEEE 802.11ad compliant.

$$G(\varphi,\theta) = G_0 - 12\cdot\left(\frac{\theta}{\theta_{3dB}}\right)^2 - 12\cdot\left(\frac{\varphi}{\varphi_{3dB}}\right)^2$$

where G_0 is an antenna gain. The horizontal and vertical half beam width are 10° in this simulation.

3.3.3.3 Channel generation

The functions of this block generate serving and interfering channels for each UE according to defined channel modelling scenario. For LTE transmissions ITU UMa/UMi channel models are used and it can be generated by SCME channel model [20]. For mm-wave transmissions "Open Area" case of channel model described in [17] is used. The time-frequency correlated channel is shown in Fig. 3.3.3.3-1.

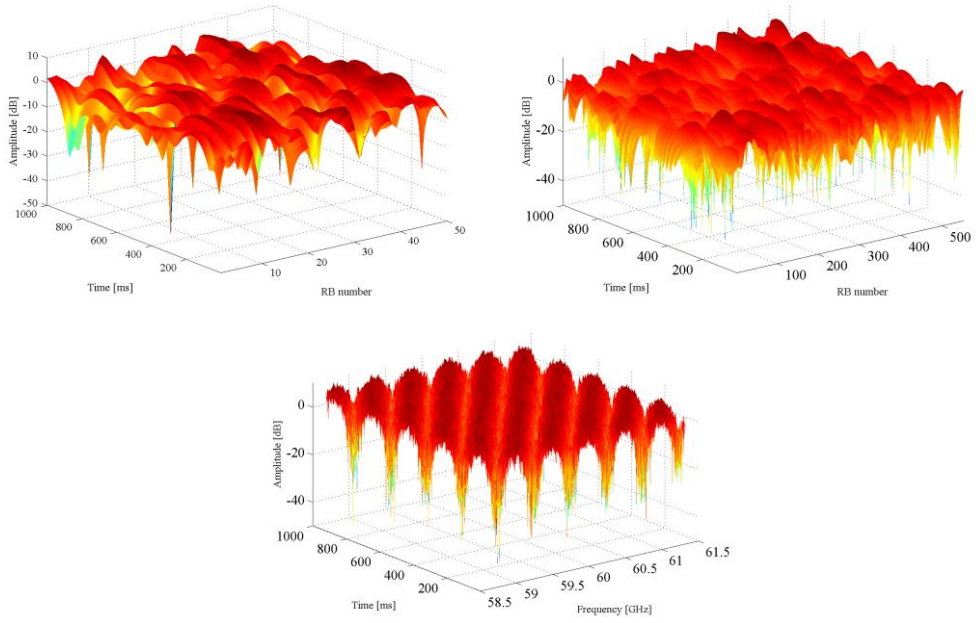

Figure 3.3.3.3-1 Time-frequency correlated channel transfer function (Left above: LTE macro, Right above: LTE small, Bottom: mm-wave small)

Moreover, since we consider time transition and UE movement, spatial correlated shadowing should be introduced. The spatial correlated shadowing is generated from uncorrelated random shadowing. From 3GPP standard [14], the distance dependent correlation coefficient follows an exponential function

$$\rho(d) = \exp\left(-\frac{d}{d_{\text{cor}}}\right),$$

where d is a distance between 2 locations and d_{cor} is a correlation distance. In order to generate 2D correlated shadowing map, we introduce horizontal/vertical filter coefficient a_k and diagonal filter coefficient b_k. If the resolution of the shadowing is d_{res}, these filter coefficients are given as follows

$$a_k = \frac{1}{\sqrt{d_{\text{cor}}}}\exp\left(-\frac{kd_{\text{res}}}{d_{\text{cor}}}\right)$$

$$b_k = \frac{1}{\sqrt{d_{\text{cor}}}}\exp\left(-\frac{k\sqrt{2}d_{\text{res}}}{d_{\text{cor}}}\right),$$

k is the running filter coefficient index. We cut the exponential decay function at maximum distance of $4d_{\text{cor}}$ and normalize each filter coefficient with $\sqrt{d_{\text{cor}}}$. We initialize the map with normal distribution value then apply these filters in horizontal, vertical and diagonal by convolutional operation as follows.

$$B_{x,y}^{[1]} = N(0,1)$$

$$B_{x,y}^{[2]} = \sum_{k=0}^{\lfloor 4d_{\text{cor}}/d_{\text{res}} \rfloor} a_k B_{x,y-k}^{[1]}$$

$$B_{x,y}^{[3]} = \sum_{k=0}^{\lfloor 4d_{\text{cor}}/d_{\text{res}} \rfloor} a_k B_{x-k,y}^{[2]}$$

$$B_{x,y}^{[4]} = \sum_{k=0}^{\lfloor 4d_{\text{cor}}/d_{\text{res}} \rfloor} b_k B_{x-k,y-k}^{[3]}$$

$$B_{x,y}^{[5]} = \sum_{k=0}^{\lfloor 4d_{\text{cor}}/d_{\text{res}} \rfloor} b_k B_{x-k,y+k}^{[4]}$$

where $B_{x,y}$ is a shadowing value of the position (x,y). After the correlation calculation, the edge area is removed and the values of the remaining map are appropriately scaled to have the desired mean value μ and standard deviation σ. The procedure of this shadowing generation is shown in Fig. 3.3.3.3-2.

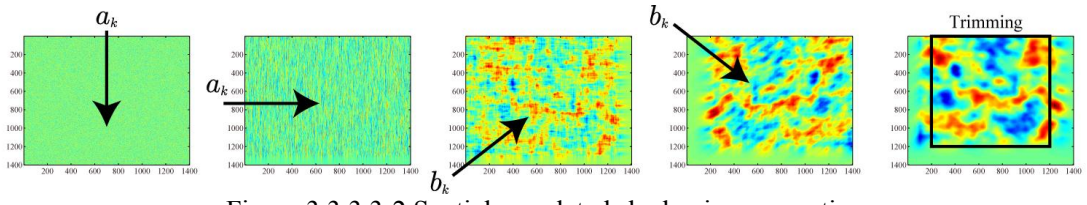

Figure 3.3.3.3-2 Spatial correlated shadowing generation

3.3.3.4 Rx processing

This block performs the receive processing for each UE using the serving and interfering channel from the previous step. The post processing SINR is used to obtain PER by means of MMIB based PHY abstraction described in Section 2.3

3.3.3.5 Feedback generation

Using knowledge about the channel state each UE calculates suitable MCS, TX antenna weights and rank indicator and reports them to its serving station.

3.3.4 System level simulator GUI

We developed system level simulator for non-full-buffer scenario by MATLAB with GUI. We can check the simulation progress visually. Figure 3.3.3.5-1 is a snapshot of the GUI.

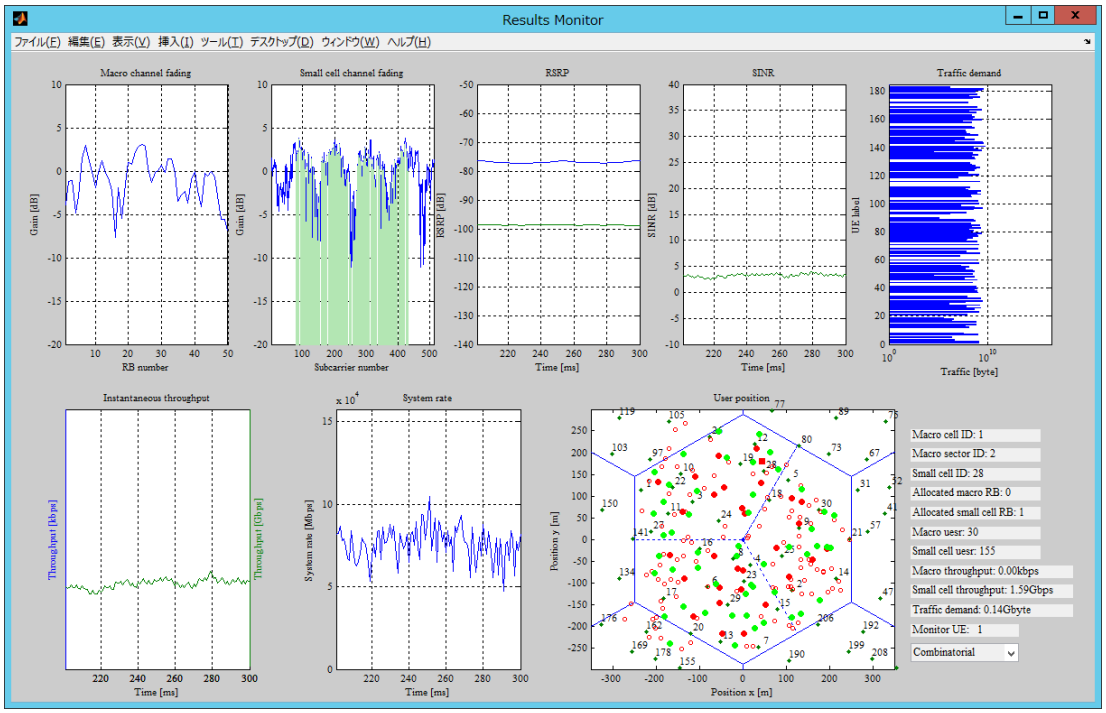

Figure 3.3.3.5-1 The SLS GUI (in non-full-buffer scenario)

Partially seen in Fig. 3.3.3.5-1, the simulator can calculate instantaneous user throughput, RSRP, RSRQ, SINR, cell throughput of each BSs, and system rate. The definition of RSRP (Reference Signal Received Power) and RSRQ (Reference Signal Received Quality) are as follows.

$$\mathrm{RSRP} = \frac{\sum(\text{Reference signal received power})}{\#\text{ of RE for reference signals}}$$

$$\mathrm{RSRQ} = \frac{\#\text{ of RB} \times \mathrm{RSRP}}{\mathrm{RSSI}}$$

$$\mathrm{RSSI} = \text{Received power of signal} + \text{interferen ce} + \text{noise}$$

4 Evaluation methodology

4.1 Evaluation factors

The purpose of this simulation is to reveal the potential of mm-wave overlay HetNet. Therefore the evaluation factors should be as follows,

- Average UE throughput
  User throughput is defined as the total amount of received data divided by the evaluation period.

$$\text{User throughput [bps]} = \frac{\min(\text{Instantaneous received data [bit]}, \text{User traffic demand [bit]})}{\text{Evaluation period [s]}}$$

  If we consider full-buffer scenario, the numerator becomes instantaneous received data. We can evaluate the average performance of the network by average user throughput.
- Cell edge UE throughput
  The definition of cell edge UE throughput is the 5 percentile value of the UE throughput CDF. Cell edge UE throughput indicates the minimal user experience of the network.
- System rate
  System rate is a sum of the user throughput within one macro cell area. It shows the total network capacity.
- System rate gain
  System rate gain is defined as the ratio of system rate between the proposed mm-wave overlay HetNet and conventional homogeneous network without small cells.

4.2 Simulator calibration

In order to calibrate the two simulators in full and non-full buffer scenarios, some factors are evaluated and compared using the developed simulators by the procedure explained in Section 3.3.1. The parameters are listed below.

TABLE 4.2-1 Simulation parameters for calibration

Parameter	Value
mm-wave Tx power [dBm]	10
Number of users per one macro cell	200
Number of smallcell BS per one macro cell	30
Traffic demand model	Full buffer

Table 4.2-2 shows numerical results derived from the two simulators. Since all results indicate almost same values, we can confirm that the two simulators have no significant difference and can be equivalently used to evaluate the potential of the proposed mm-wave overlay HetNet. The slight difference is mainly caused by the difference of user association method.

TABLE 4.2-2 Calibration results

		BS throughput, [Mbps]	**Avg. UE throughput, [Mbps]**	**Cell edge UE throughput, [Mbps]**	**Assigned UEs, %**
EU	LTE	20.9	1.04	0.39	10.1
	mm-wave	3714	619.4	62.4	89.9
	joint	111441	557.2	0.9	100
JP	LTE	35.8	2.35	0.17	19.4
	mm-wave	4777	885.1	2.67	80.6
	joint	143430	775.3	1.24	100

5 Preliminary evaluation results

5.1 Performance comparison of mm-wave overlay HetNet (Full-buffer scenario)

5.1.1 Mm-wave overlay HetNet deployment in Europe and Japan

In this Section we will compare performance of mm-wave HetNet deployment in full-buffer model for two cases in Europe and Japan. Unlike the European regulations where the maximum EIRP for mm-wave frequencies is limited by 57 dBm, there is stronger requirement to the emitted power in Japan. This limit is equal to 10 dBm only. Therefore the regulator requirements lead to denser mm-wave small cell deployment for Japan scenario under assumption of constant UE density. In order to achieve similar SNR for cell edge UEs, in our simulations we have reduced small cell radius for Japan scenario by factor 2.5 in comparison with European scenario, as illustrated in Figure 5.1.1-1.

Figure 5.1.1-1 Deployment scenarios for Europe and Japan

5.1.2 Deployment of mm-wave small cells in the Macro LTE cell

In practical deployments mm-wave small cells are randomly dropped in hotspots inside of Macro Cell area (see Figure 5.1.2-1). But for initial performance evaluation we will consider only two extreme cases:

- **"**Isolated cell". In this case small cell are dropped so rarely that we can neglect interference between them and estimate the overlay mm-wave network performance through simulating only one mm-wave small cell.
- "Dense hexagonal deployment". In this opposite extreme case mm-wave HetNet deployment has maximal density and therefore the maximal inter-cell interference is achieved.

It should be note that all other mm-wave HetNet deployments will have performances between these two extreme cases.

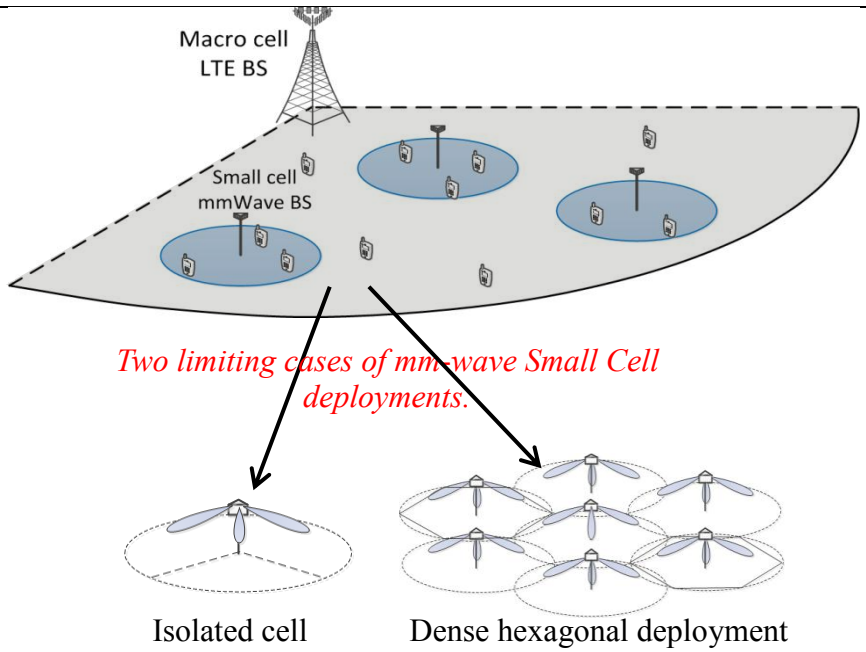

Figure 5.1.2-1 Deployment of mm-wave HetNets in the Macro LTE cell

5.1.3 System level simulations results.

The overlay mm-wave HetNets parameters used for simulations are presented in Table 5.1.3-1.

Table 5.1.3-1 mm-wave simulation parameters

Parameters		Assumption
Deployment / Traffic load		Isolated single cell, Dense hexagonal / Full-buffer
Bandwidth / Frequency reuse		2 GHz / 3
Cell radius / Number of UEs per cell*		**20 m(JP), 50m (EU) / 8(JP), 50(EU)**
BS/UE antenna height		4 m / 1.5 m
Transmission scheme		MU-MIMO
Channel model		LOS. Free space+O_2 absorption (15dB/km) pathloss
Link adaptation	Outer loop target FER	10 %
Scheduling	Type	Proportional-fair MU greedy scheduling
BS antenna element	Element gain/Front2Back	5 dBi/12 dB
	Horizontal/Vertical beamwidth	80°/80°
BS antenna array	Configuration/TX power*	8x32 elements / **10dBm(JP), 22dBm(EU)**
	Array model	Full adaptive antenna array
UE antenna		Single element, omni-directional

*The parameters marked by red(JP) and by blue(EU) are for Japanese and European scenarios respectively

The main simulation results in full-buffer scenario obtained using the developed system level simulation platform are presented in Table 5.1.3-2 and Figures 5.1-3.

Table 5.1.3-2 mm-wave simulation results

Scenario	Small cell BS throughput, [Gbps]	Avg. UE throughput, [Mbps]	Cell edge UE throughput, [Mbps]
EU isolated cell	27.0	540	315
JP isolated cell	13.6	1695	927
EU dense deployment	14.9	297	142
JP dense deployment	7.0	876	379

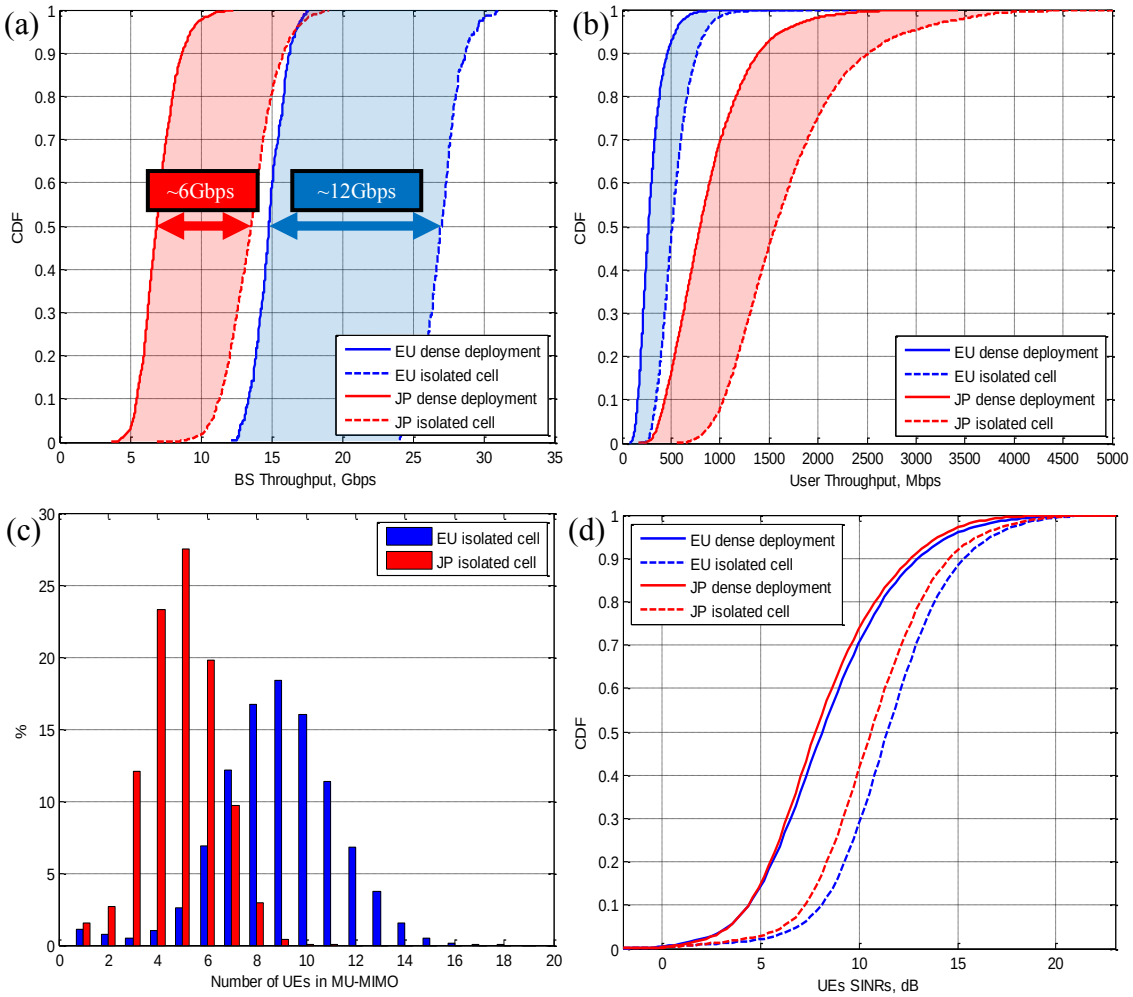

Figure 5.1.3-1 Full-buffer simulation results. a) BS throughput CDF; b) UE throughput CDF; c) Number of UEs in MU-MIMO; d) UEs SINR CDF.

The results presented in Table 5.1.3-2 show that densification of smallcell BS in Japan scenario by 5-6 times in comparison with Europe scenario leads to 3 times higher average and cell edge UE throughputs for given area.

From comparison of two extreme cases: Isolated Cell, Dense Hexagonal deployment (see CDF BS throughput curves on Figure 5.1.3-1(a)) the maximal inter-cell interference impact may be estimated: 6Gbps in Japanese and about 12Gbps in European scenarios. Therefore the implementation of modern interference mitigation schemes (e.g. CoMP, ICIC) may lead to substantial overlay mm-wave system

performance improvement (see for example [21]). More details about mmWave HetNet systems performance evaluations can be found in [22].

5.2 Performance comparison of mm-wave overlay HetNet (Non-full-buffer scenario)

We evaluate the factors which are listed in Section 4.1 by using our developed simulator in non-full-buffer scenarios. Simulation execution parameters for the non-full-buffer scenario are shown in Table 5.2-1, noting that in order to alleviate the scheduler warming up effect, the first 100ms results are discarded.

TABLE 5.2-1 Simulation Parameters

Parameter	Value
Evaluation period [ms]	1000 (discard first 100ms results)
Number of users per one macro cell	200 (slightly changed by simulation condition)
Number of smallcell BS per one macro cell	50
Average traffic demand [Mbyte]	62
Cell association method	Combinatorial

The simulation results are summarized in Table 5.2-1

TABLE 5.2-1 Simulation Results

Network	System rate	Average user rate	Cell edge (outage) user rate	System rate gain
HomoNet	121.46 Mbps	656.56 kbps	183.30 kbps	
HetNet (w/o MU-MIMO)	117010 Mbps	632.46 Mbps	587.19 kbps	963
HetNet (w/ MU-MIMO)	153580 Mbps	830.16 Mbps	1.26 Mbps	1264

In this realistic non-full-buffer simulation, we can obtain about 1000 times gain by installing 50 mm-wave small cell BSs. By introducing MU-MIMO technology, we can achieve a system rate gain of 1264 times since many users can obtain ultra-high speed transmission simultaneously. Also MU-MIMO can improve the average user throughput and the outage user rate.

6 References

[1] E. Tuomaala and H. Wang, "Effective SINR approach of link to system mapping in OFDM/multi-carrier mobile network," *in Proc. Int. Conf. Mobile Tech., Appl. Syst.,* Nov. 2005.

[2] 3GPP TS 36.211, "Evolved Universal Terrestrial Radio Access (E-UTRA); Physical channels and modulation".

[3] 3GPP TS 36.212, "Evolved Universal Terrestrial Radio Access (E-UTRA); Multiplexing and channel coding".

[4] 3GPP TS 36.213, "Evolved Universal Terrestrial Radio Access (E-UTRA); Physical layer procedures".

[5] E. Dahlman, S. Parkval and J. Skold, "4G: LTE/LTE-Advanced for Mobile Broadband: LTE/LTE-Advanced for Mobile Broadband," *Academic Press,* May 2011.

[6] J. C. Ikuno, S. Schwarz and M. Simko, "LTE Rate Matching Performance with Code Block Balancing," *in Proc. European Wireless Conference (EW),* 2010.

[7] "Enhancements for Very High Throughput in the 60GHz Band," *IEEE 802.11ad standard.*

[8] "IEEE 802.11ad Amendment 3: Enhancements for Very High Throughput in the 60 GHz Band," 2012.

[9] "Channel Models for 60 GHz WLAN Systems," *IEEE 802.11 doc. 0334r8.*

[10] "Implementation of 60 GHz WLAN Channel Model," *IEEE 802.11 doc. 0854r3.*

[11] K. Sayana, J. Zhauang and K. Stewart, "Short term link performance modeling for ML receivers with mutual information per bit metrics," *Proc. IEEE GLOBECOM 2008,* Nov. 2008.

[12] G. Caire, "Bit-Interleaved Coded Modulation," *IEEE Transactions on Information Theory,* vol. 44, no. 3, May 1998.

[13] J. Kim, A. Ashikhmin, A. de Lind van Wijngaarden, E. Soljanin and N. Gopalakrishnan, "Reverse Link Hybrid ARQ: Link Error Prediction Methodology Based on Convex Metric," *3GPP2 TSG-C WG3 20030401-020,* 1 April 2003.

[14] 3GPP TR 36.814, "Further advancements for E-UTRA physical layer aspects".

[15] 3GPP TR 36.872, "Small cell enhancements for E-UTRA and E-UTRAN - Physical layer aspects".

[16] MiWEBA Deliverable D3.1, "Separation of data and control plane".

[17] MiWEBA Deliverable D5.1, "Channel Modeling and Characterization".

[18] H. Shimodaira, G. K. Tran, K. Araki, K. Sakaguchi, S. Nanba, T. Hayashi and S. Konishi, "Cell Association Method for Multiband Heterogeneous Networks," *Personal, Indoor and Mobile Radio Communications (PIMRC Workshops), 2014 IEEE 25th International Symposium on,* Sep. 2014.

[19] P. Viswanath, D. Tse and R. Laroia, "Opportunistic beamforming using dumb antennas," *IEEE Transactions on Information Theory,* vol. 48, pp. 1277-1294, 2002.

[20] D. S. Baum, J. Salo, M. Milojevic, P. Kyösti and J. Hansen, "MATLAB implementation of the interim channel model for beyond-3G systems (SCME)," May 2005. [Online]. Available: http://www.tkk.fi/Units/Radio/scm/.

[21] G.V. Morozov, A.V. Davydov, A.A. Maltsev, "Analysis of the throughput of the cellular radio-communication systems using coordinated data transmission to suppress mutual unintended interference," *Radiophysics and Quantum Electronics,* vol. 57, no. 3, pp. 226-238, 2014.

[22] A. Maltsev, A. Sadri, A. Pudeyev, R. Nicholls, R. Arefi, A. Davydov, I. Bolotin, G. Morozov, K. Sakaguchi and T. Haustein, "MmWave Smallcells is a Key Technology for Future 5G Wireless Communication Systems," in *European Conference on Networks and Communications (EuCNC'2014)*, Bologna, 2014.